JBC ARTICLE

High phosphatidylinositol 4-phosphate (PI4P)-dependent ATPase activity for the Drs2p-Cdc50p flippase after removal of its N- and C-terminal extensions

Received for publication, August 2, 2016, and in revised form, March 10, 2017 Published, Papers in Press, March 16, 2017, DOI 10.1074/jbc.M116.751487

Hassina Azouaoui[‡], Cédric Montigny[‡], Thibaud Dieudonné[‡], Philippe Champeil[‡], Aurore Jacquot[‡], José Luis Vázquez-Ibar[‡], Pierre Le Maréchal[§], Jakob Ulstrup[¶], Miriam-Rose Ash[¶], Joseph A. Lyons[¶], Poul Nissen[¶], and Guillaume Lenoir[‡1]

From the [‡]Institute for Integrative Biology of the Cell (I2BC), CEA, CNRS, Université Paris-Sud, Université Paris-Saclay, F-91198, Gif-sur-Yvette Cedex, France, the [§]Neuro-PSI-UMR CNRS 9197, Bâtiment 430, Université Paris-Sud, Université Paris-Saclay, 91405 Orsay Cedex, France, and the [¶]DANDRITE, Nordic-EMBL Partnership for Molecular Medicine, and PUMPkin, Department of Molecular Biology and Genetics, Danish National Research Foundation, Aarhus University, Gustav Wieds Vej 10C, 8000 Aarhus C, Denmark

Edited by Dennis R. Voelker

P4-ATPases, also known as phospholipid flippases, are responsible for creating and maintaining transbilayer lipid asymmetry in eukaryotic cell membranes. Here, we use limited proteolysis to investigate the role of the N and C termini in ATP hydrolysis and auto-inhibition of the yeast flippase Drs2p-Cdc50p. We show that limited proteolysis of the detergent-solubilized and purified yeast flippase may result in more than 1 order of magnitude increase of its ATPase activity, which remains dependent on phosphatidylinositol 4-phosphate (PI4P), a regulator of this lipid flippase, and specific to a phosphatidylserine substrate. Using thrombin as the protease, Cdc50p remains intact and in complex with Drs2p, which is cleaved at two positions, namely after Arg^{104} and after Arg ^{1290}, resulting in a homogeneous sample lacking 104 and 65 residues from its N and C termini, respectively. Removal of the 1291–1302-amino acid region of the C-terminal extension is critical for relieving the auto-inhibition of full-length Drs2p, whereas the 1–104 N-terminal residues have an additional but more modest significance for activity. The present results therefore reveal that trimming off appropriate regions of the terminal extensions of Drs2p can greatly increase its ATPase activity in the presence of PI4P and demonstrate that relief of such auto-inhibition remains compatible with subsequent regulation by PI4P. These experiments suggest that activation of the Drs2p-Cdc50p flippase follows a multistep mechanism, with preliminary release of a number of constraints, possibly through the binding of regulatory proteins in the *trans*-Golgi network, followed by full activation by PI4P.

Transbilayer lipid movement is essential to many aspects of cell function. For example, for proper expansion of biogenic membranes like the ER[2] membrane, translocation of phospholipids toward the luminal leaflet must accompany synthesis on the cytosolic leaflet (1). Energy-independent lipid transporters generally referred to as phospholipid "scramblases" fulfill this activity (2–4). In contrast to these phospholipid scramblases, which equilibrate lipid concentrations in a relatively nonspecific manner over the two leaflets of biological membranes, active transporters termed "flippases" use the chemical energy of ATP to catalyze uphill transport of specific lipids, thereby creating and maintaining phospholipid asymmetry in the membranes in which they are embedded. One of the most prominent lipids actively transported by flippases is phosphatidylserine (PS), which is enriched in the cytosolic leaflet of membranes from the late secretory/endocytic pathways. PS asymmetry is critical for cell life as signaling proteins that contain stretches of basic residues, such as K-Ras, use the negatively charged headgroup of PS lipids as a docking site (5, 6). Also, PS is the target of C2 domain-containing proteins like protein kinase C and synaptotagmin, respectively involved in protein phosphorylation and membrane fusion. Conversely, dissipation of PS asymmetry at the plasma membrane is an early and very potent apoptotic signal that triggers recognition by macrophages (7).

Phospholipid flippases belong to the P4 subfamily of P-type ATPases (P4-ATPases) (8), and mutations of some of the mammalian P4-ATPases are associated with pathological conditions. For instance, mutations in ATP8B1 are directly linked to intrahepatic cholestasis, a liver disease that in severe forms may progress toward liver failure and death before adulthood (9), whereas ATP8A2 mutations are causative of the rare cerebellar ataxia, mental retardation, and disequilibrium syndrome (10).

Although the molecular mechanism of phospholipid transport through P4-ATPases has drawn much attention in the recent years (11, 12), little is known about how lipid flippases

This work was supported by the CNRS, by Agence Nationale de la Recherche (ANR) Grant ANR-14-CE09-0022 (to G. L.) (AsymLip), by French Infrastructure for Integrated Structural Biology (FRISBI) Grant ANR-10-INSB-05, and by Postdoctoral Fellowship R171-2014-663 from the Lundbeck Foundation (to J. A. L.). The authors declare that they have no conflicts of interest with the contents of this article.

[1] To whom correspondence should be addressed: Institute for Integrative Biology of the Cell, Bâtiment 528, PC 103, CEA Saclay, 91191 Gif-sur-Yvette Cedex, France. Tel.: 33-169087589; Fax: 33-169088139; E-mail: guillaume.lenoir@i2bc.paris-saclay.fr.

[2] The abbreviations used are: ER, endoplasmic reticulum; TGN, *trans*-Golgi network; SERCA1a, sarco/ER Ca^{2+}-ATPase, isoform 1a; DDM, *n*-dodecyl β-D-maltoside; POPS, 1-palmitoyl-2-oleoyl-*sn*-glycero-3-phosphoserine; PI4P, phosphatidylinositol 4-phosphate; $PI(4,5)P_2$, phosphatidylinositol-4,5-bisphosphate; NBD, 7-nitrobenz-2-oxa-1,3-diazol-4-yl; TEMED, *N,N,N′, N[prime]*-tetramethylethylenediamine; TEV, tobacco etch virus; PS, phosphatidylserine; SEC, size-exclusion chromatography; TED, tris(carboxymethyl)ethylenediamine; mAU, milli-absorbance.

work. Recent studies with a yeast flippase suggested that lipids flip across the membrane through a peripheral pathway, along the protein/lipid interface (13, 14). However, this view was challenged by studies on another phospholipid-translocating P4-ATPase, the mammalian ATP8A2-CDC50A complex, suggesting that the lipid headgroup-binding site might be more deeply buried into the ATPase helix bundle (15).

Drs2p, a yeast flippase, is one of the most intensively studied P4-ATPases. Drs2p specifically interacts with Cdc50p, a glycosylated membrane protein that is required for ER exit of the flippase complex (16, 17) and that is proposed to play an intimate role in the transport cycle of Drs2p (18, 19). When embedded in TGN membranes, Drs2p has been shown to translocate fluorescently labeled PS (*i.e.* PS bearing an NBD fluorescent moiety on one of its acyl chains) at the energetic expense of ATP hydrolysis (20, 21). Such NBD-PS transport activity has been further demonstrated after purification and reconstitution into proteoliposomes (22).

Up to now, only a few laboratories have succeeded in purifying a Drs2p-Cdc50p complex and to assay its ATPase activity (22, 23). This activity was found to be strictly dependent on phosphatidylinositol 4-phosphate (PI4P) (23), but also to be remarkably low compared with those of the ATP8A2-CDC50A complex (24) or several P2-type ATPases, like the prototypic and thoroughly studied ion-translocating Na^+/K^+- or Ca^{2+}-ATPases.

P4-ATPases are predicted to contain 10 transmembrane spans and a large cytosolic region. The cytosolic region is made of three distinct pieces as follows: the nucleotide-binding (N) domain binds ATP; the phosphorylation (P) domain is phosphorylated from ATP during the transport cycle; and the actuator (N) domain contains a strongly conserved motif involved in the dephosphorylation of the P domain (Fig. 1*A*). Compared with ATP8A2 and with most P2-ATPases, Drs2p contains relatively long N- and C-terminal extensions of up to ~190–200 amino acids on the N-side and ~130–140 amino acids on the C-side (Fig. 1*A*), to which various regulators of Drs2p are known to bind. The Arf-like protein Arl1p interacts with the N terminus of Drs2p, stimulating Drs2p ATPase activity in purified TGN membranes (25). In addition, both the guanine nucleotide exchange factor protein Gea2p and PI4P regulate the activity of Drs2p upon binding to its C terminus (26, 27). Remarkably, a recent study suggested that the C-terminal tail of Drs2p exerts an auto-inhibitory effect on Drs2p activity, an auto-inhibition that would be relieved by binding of PI4P (28). Indeed, a relatively common feature of a number of P-type ATPases (*e.g.* plasma membrane Ca^{2+}-ATPases and H^+-ATPases) is that N- and/or C-terminal extensions of a central core structure contribute significant auto-inhibition to the full-length protein activity, with regulators often releasing such auto-inhibition by binding to these peripheral extensions and thereby relieving their impact on binding events and domain movements required for catalytic activity (29–32).

We earlier attempted[3] to overexpress, together with Cdc50p, a number of truncated variants of Drs2p, in which portions of the Drs2p N or C terminus had been deliberately deleted. However, C-terminally truncated variants of Drs2p were poorly expressed and solubilized from yeast membranes, and the glycosylation pattern of the co-expressed Cdc50p was altered, suggesting that C-terminal truncation of Drs2p has a deleterious impact on Drs2p-Cdc50p association. Obviously, such attempts may suffer from the possibility that one does not necessarily guess correctly at which exact point truncation should be performed for relieving auto-inhibition without inducing collateral effects. As an alternative approach, we submitted the purified full-length Drs2p-Cdc50p complex to limited proteolysis, anticipating that the presumably poorly structured Drs2p extensions would be more susceptible to proteolysis than the well organized domains of its central core and that limited proteolysis under appropriate conditions would allow us to investigate the functional properties of a complex devoid of its regulatory extensions.

Here, we show that thrombin treatment of the purified Drs2p-Cdc50p complex in the presence of PI4P results in the formation of a polypeptide devoid of the first 104 N-terminal residues and of the last 65 C-terminal residues. We found that such truncation of Drs2p stimulates ATPase activity to a very large and previously unrecognized extent, namely by 10–20-fold (30–50-fold when trypsin is used as the protease). Remarkably, stimulation of ATPase activity remains strongly dependent on PI4P, even though truncation of the C-terminal region occurred in the vicinity of the predicted PI4P-binding site. Our data demonstrate that full activation of Drs2p-Cdc50p by PI4P is not mediated through a simple PI4P-induced displacement of the whole C-terminal tail. Instead, we propose a multistep mechanism where the C-terminal tail of Drs2p, in cooperation with the N terminus, must be displaced before PI4P can exert its full stimulatory role.

Results

Limited proteolysis in the presence of PI4P of purified Drs2p-Cdc50p dramatically increases its ATP hydrolysis rate

Because secondary structure predictions suggest that the N and C termini of Drs2p are intrinsically disordered, our rationale was that limited proteolysis might be a convenient tool to remove these possible auto-inhibitory extensions. Therefore, we subjected the purified Drs2p-Cdc50p complex to such proteolysis and monitored its ATPase activity using a continuous assay based on NADH oxidation by a regenerating system (33).

As illustrated in Fig. 1*B*, the activity of an intact purified Drs2p-Cdc50p complex was first assayed in the presence of PI4P, which has been shown to be essential for activation of this intact complex (23). As expected, the rate of NADH absorption changes resulting from its very low ATPase activity was only slightly different from the background rate of NADH absorption changes. Note that although this PI4P-stimulated activity was hardly distinguishable from the background noise using the NADH assay, it could be unambiguously measured with a larger protein concentration using a phosphomolybdate procedure (Fig. 1*D*) (23). When the Drs2p-Cdc50p complex had been treated beforehand with trypsin, a much higher rate of NADH oxidation showed up, implying activation of the complex by

[3] H. Azouaoui, A. Jacquot, C. Montigny, P. Champeil, and G. Lenoir, unpublished results.

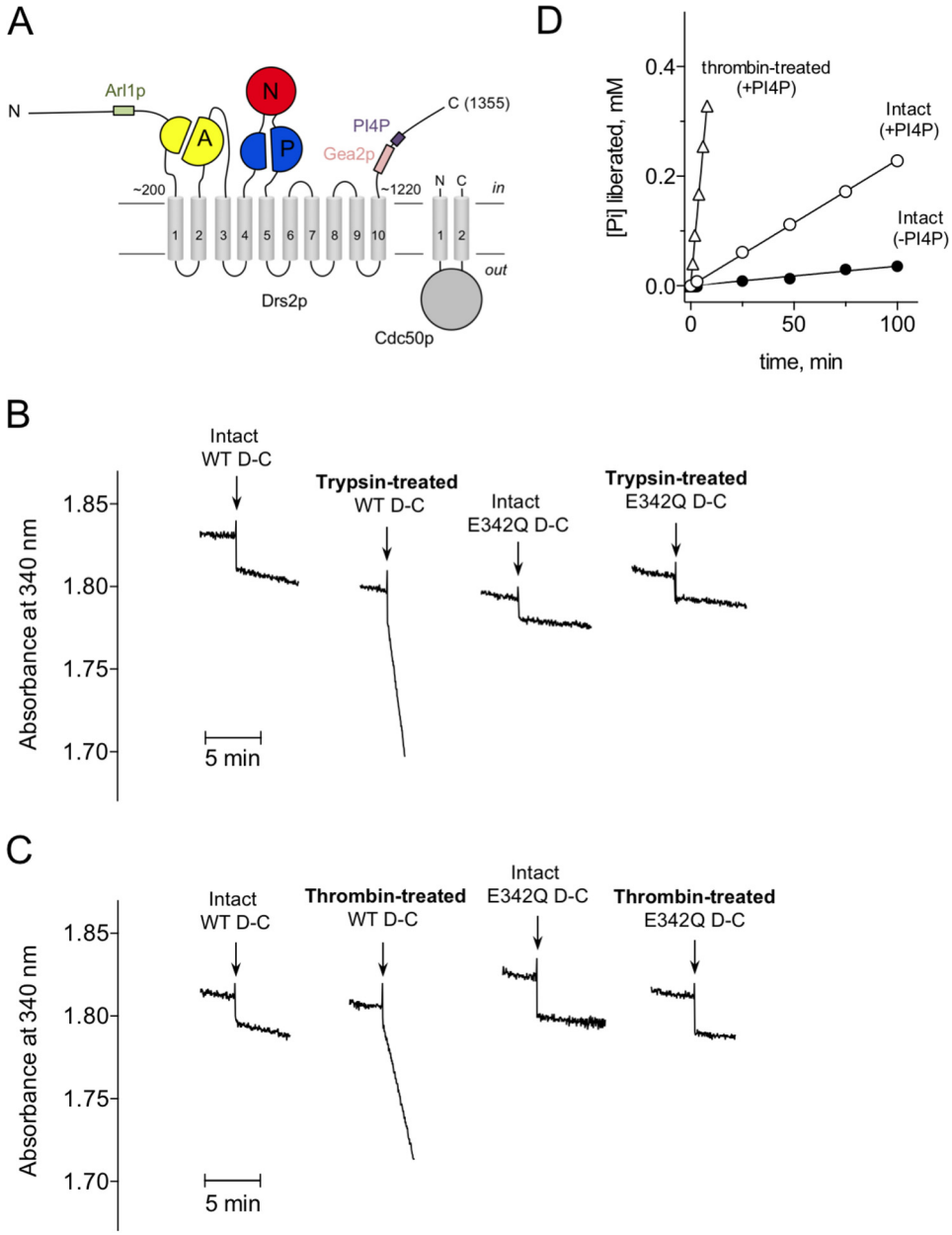

Figure 1. Proteolysis by either trypsin or thrombin in the presence of PS and PI4P, of the purified Drs2p-Cdc50p complex, dramatically increases its ATP hydrolysis rate. *A*, schematic representing the predicted topology of Drs2p and Cdc50p. The cytosolic actuator (*A, yellow*), nucleotide-binding (*N, red*), and phosphorylation (*P, blue*) domains, as well as the transmembrane helices (*gray cylinders*), are indicated. The binding sites for Arl1p, Gea2p, and PI4P are represented. *B*, ATPase activity was measured using an enzyme-coupled assay, at 30 °C. The purified Drs2p-Cdc50p (D-C) complex, either WT or the E342Q inactive mutant, was added at a final concentration of ~5 μg/ml protein to continuously stirred optical assay cuvettes containing 1 mg/ml DDM, 0.05 mg/ml POPS, 0.025 mg/ml PI4P, and 1 mM Mg^{2+}-ATP in SSR buffer in the presence of a regenerating system. When indicated, the purified complex had been pre-treated with 40 μg/ml trypsin for 1 h at 20 °C in the presence of 0.025 mg/ml PI4P and 0.05 mg/ml POPS. *C*, same as *B*. but in this case the purified complex had been pre-treated with 40 units/ml (~20 μg/ml) thrombin, also for 1 h at 20 °C in the presence of 0.025 mg/ml PI4P and 0.05 mg/ml POPS. *B* and *C*, the drift in NADH absorption before addition of the ATPase was mainly due to photobleaching of NADH (see "Experimental procedures"). The traces shown in *B* and *C* are representative of several independent ones with similar results. *D*, ATPase activity measurements with intact and thrombin-treated samples, using the molybdate assay. Intact (*circles*) and thrombin-treated (*triangles*) samples were diluted 3-fold, and ATPase activity was measured in the absence (*closed symbols*) or presence (*open symbols*) of 0.025 mg/ml PI4P. Note that due to the too high residual PI4P concentration after 3-fold dilution, the ATPase activity of the thrombin-treated sample in the absence of PI4P could not be measured with this technique. Complementary experiments addressing the PI4P dependence of the activity of this sample are reported in Fig. 5. In all cases the assay medium (in the absence of regenerating system) was supplemented with 1 mg/ml DDM and 0.05 mg/ml PS.

proteolysis (Fig. 1*B*). The observed effect was specifically associated with Drs2p activation, as treatment with trypsin of the inactive E342Q mutant of Drs2p did not result in any increase of its activity (Fig. 1*B*). The specific ATPase activity was stimulated about 30–50-fold after trypsin treatment, increasing from ~0.03–0.07 to ~ 1.5–2.0 μmol·min^{-1}·mg^{-1}.

Pre-treatment of the Drs2p-Cdc50p complex with thrombin also led to a large increase in ATPase activity, although to a slightly lower level (Fig. 1, *C* and *D*). When other proteases were used in the presence of PI4P, like chymotrypsin or the poorly specific proteinase K and subtilisin proteases, stimulation of the ATPase activity of the purified complex was also observed,

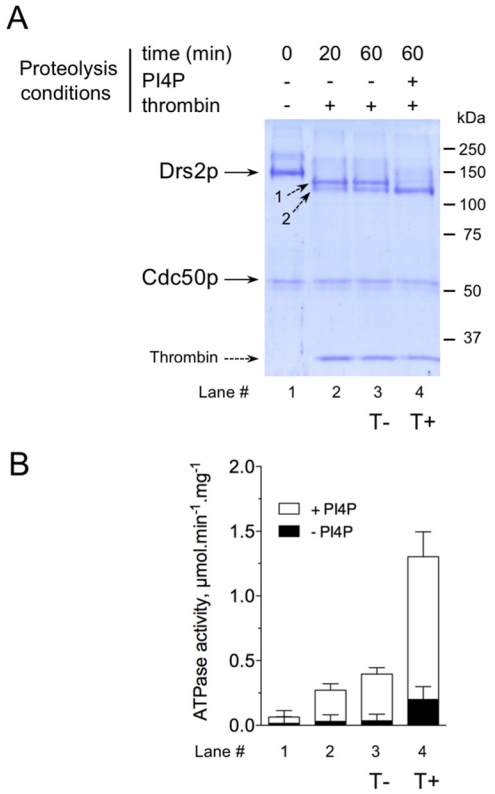

Figure 2. Limited proteolysis of purified Drs2p-Cdc50p results in transient accumulation of two major types of Drs2p long fragments, with increased and PI4P-sensitive overall activity. To the purified WT Drs2p-Cdc50p complex at about 0.2 mg/ml protein in SSR buffer containing 0.5 mg/ml DDM and 0.025 mg/ml POPS, additional DDM and POPS was added, up to 1 and 0.05 mg/ml, respectively, together or not with PI4P at 0.025 mg/ml. Proteolysis (at 20 °C) was triggered by addition of thrombin at a final concentration of 40 units/ml. Proteolysis took place for either 20 or 60 min, in the latter case in the absence or presence of PI4P, before quenching with PMSF and liquid nitrogen freezing. *A*, 2 μg of the proteolyzed samples were loaded onto an 8% SDS-PAGE for Coomassie Blue staining of the resulting polypeptides. The two bands observed for Cdc50p correspond to different glycosylation levels. *B*, ATPase activity was measured by an enzyme-coupled assay, by diluting samples into a 2-ml SSR assay medium containing 0.75 mg/ml DDM, 0.05 mg/ml POPS, 1 mM Mg^{2+}-ATP, and an ATP-regenerating system, in the presence (*open bars*) or absence (*closed bars*) of 0.025 mg/ml PI4P. When cleavage had been performed in the presence of PI4P (*lane 4*), the activity plotted as the one in its absence was recorded after allowing for extensive PI4P dissociation into a PI4P-free assay medium (see Fig. 5). This figure shows one representative experiment of several independent ones with similar results.

although to various extents (data not shown), suggesting that the portions of the Drs2p-Cdc50p complex attacked by the various proteases are indeed especially exposed or disordered and that the remaining proteolysis fragments displaying high ATPase activity are fairly resistant to further degradation.

Limited proteolysis of Drs2p-Cdc50p by thrombin results in transient accumulation of two major Drs2p fragments with increased PI4P-sensitive ATPase activity

A specific feature of proteolysis by thrombin *versus* proteolysis by other proteases is that Cdc50p remains intact under these conditions (Fig. 2*A*). In the rest of this study, we therefore resorted to thrombin to investigate the effect of proteolysis-dependent truncation on Drs2p-Cdc50p function. After proteolysis was quenched, the proteolyzed samples were used for studying their electrophoretic migration pattern as well as for determining their ATPase activity.

Fig. 2*A* shows results selected from a number of different combinations of proteolysis periods and temperatures. In the absence of PI4P, proteolysis of the ~150-kDa full-length Drs2p chain led to transient accumulation of large fragments (named fragments 1 and 2), with little if any accumulation of smaller fragments in the 30–100-kDa range. Extending the proteolysis period from 20 to 60 min (*lanes 2* and *3* in Fig. 2*A*) slightly favored disappearance of the larger fragments ("1") and accumulation of the smaller fragments ("2"), suggesting that the latter is relatively resistant to proteolysis. Interestingly, the presence of PI4P during proteolysis strongly favored formation of the smaller fragment (*lanes 3* and *4* in Fig. 2*A*).

Irrespective of whether proteolysis was performed in the absence or presence of PI4P (samples named T− and T+, respectively), the activity of wild-type Drs2p-Cdc50p in the presence of PI4P increased very significantly compared with the very low ATPase activity of the untreated complex (Fig. 2*B*). Yet activation of the proteolyzed sample was maximal when proteolysis had occurred in the presence of PI4P, in line with an increase of the fragment 2 species (*T+ sample* in Fig. 2, *A* and *B*).

Identification of the thrombin-derived proteolytic fragments

We first analyzed the proteolysis products using N-terminal sequencing (*left panels* in Fig. 3). For untreated purified Drs2p, N-terminal residues were identified as G*X*G*X*GMND, in line with the fact that in our construct, four additional linking glycines together with one glycine from the TEV site are present upstream of the first residue. As to the bands resulting from proteolysis with thrombin (fragments 1 and 2 in T− and fragment 2 in T+), their N-terminal first amino acids were identified as being ^{105}AVKPP for both fragments 1 and 2. All thrombin-derived fragments therefore start at the same location, Ala^{105}, immediately after Arg^{104}. Although cleavage after Arg^{104} fits with the generally accepted view that thrombin only cleaves polypeptides after an arginine, the present cleavage site (. . . QSLR ↓ AVKPP. . . .) deviates significantly from the LVPR ↓ GS consensus sequence.

To estimate the exact molecular masses of Drs2p fragments 1 and 2 and thereby identify the sites of C-terminal cleavage, the thrombin-derived samples were further purified on a size-exclusion chromatography (SEC) column and submitted to MALDI-TOF analysis (*right panels* in Fig. 3). In all cases, mass spectra revealed a major peak at 52.3 ± 0.1 kDa, likely reflecting glycosylated Cdc50p.

For untreated samples, the mass spectrum also displayed a peak at an m/z value close to the one expected for full-length Drs2p, m/z ~153.9 kDa (theoretical mass = 154.0 kDa), as well as a peak corresponding to the doubly charged polypeptide (z = 2) at m/z ~77.0 kDa. For T− samples, the mass spectrum revealed a large component at an m/z of ~141.6 kDa, as well as the companion peak (for z = 2) at m/z ~70.9 kDa. As the calculated mass for the Ala^{105}–Ile^{1355} polypeptide is 141.9 kDa, this component in T− samples fits with fragment 1 resulting from a unique truncation of Drs2p at N-terminal position 105, *i.e.* left untouched at its C terminus.

For T+ samples, a major component was found at m/z ~134.5 kDa, with the companion peak (for z = 2) at m/z ~67.3

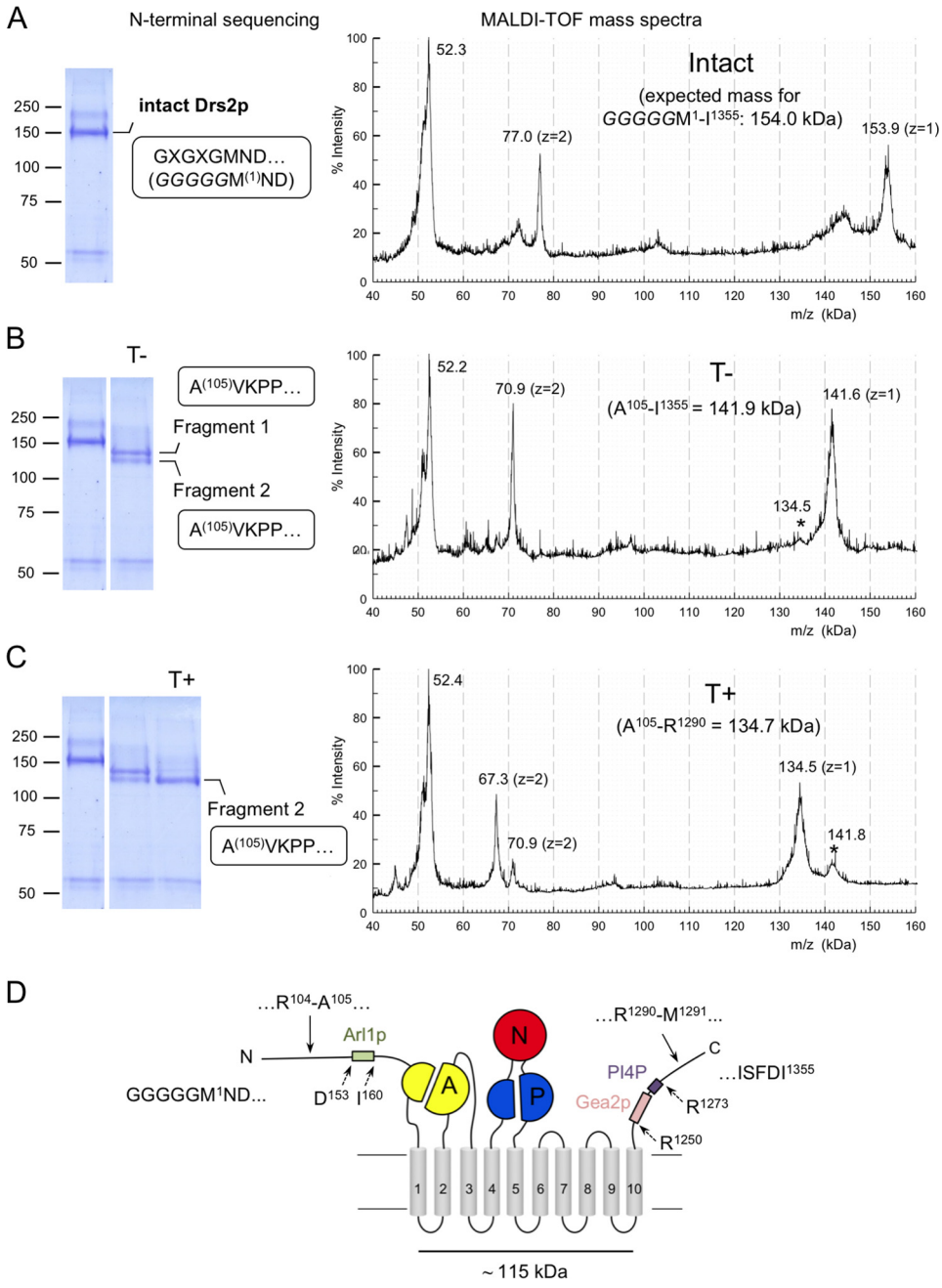

Figure 3. Identification of the fragments resulting from thrombin cleavage. N-terminal sequencing (*left*) and MALDI-TOF mass spectrometry results (*right*), together with deduced sequences and corresponding calculated masses of the main fragments, for an intact purified Drs2p-Cdc50p complex (*A*), a T− sample (*B*), and a T+ sample (*C*) are shown. Note that the masses found for these fragments are slightly different from what would be inferred from the electrophoretic pattern. *D*, schematic illustrating the location of the thrombin cleavage sites on the Drs2p chain, as well as the boundaries of the Gea2p/PI4P-binding sites (Arg^{1250}–Arg^{1273}) and a sequence of Drs2p critical for interaction with Arl1p (Asp^{153}–Ile^{160}). The data plotted represent a typical experiment of two independent ones.

kDa. Assuming that thrombin cleavage occurs after an arginine, and considering the N-terminal residue of fragment 2 (Ala^{105}) as well as the limited number of arginine residues in the C-terminal region of Drs2p, the conclusion is that fragment 2 in the T+ sample must end at Arg^{1290}, the calculated mass of which is 134.7 kDa. Indeed, the arginine residues closest to Arg^{1290} in Drs2p sequence are Arg^{1273} and Arg^{1298}, and masses for polypeptides ending at those residues would be 132.8 and 135.7 kDa, respectively, well beyond experimental error. Note that the mass spectrum of the T+ sample reveals a minor peak at ~141.8 kDa, presumably corresponding to the small amount of fragment 1 in T+, and the mass spectrum of the T− sample also reveals a minor peak at ~134.5 kDa, presumably corresponding to the small amount of fragment 2 in T−.

Hence, a consistent picture appears to be as follows (Fig. 3*D*); regardless of the presence or absence of PI4P during cleavage, thrombin treatment removes the N-terminal region of Drs2p after residue Arg^{104}. In the absence of PI4P, the primary product is mainly cleaved at the N terminus only, and has a molecular mass of 141.9 kDa (*fragment 1* in Fig. 2*A*). In the presence of

PI4P, the primary product is cleaved both at the N terminus after residue Arg^{104} and at the C terminus after residue Arg^{1290}, producing an Ala^{105}–Arg^{1290} polypeptide whose molecular mass is 134.7 kDa (*fragment 2* in Fig. 2*A*). The main Drs2p polypeptide in T+ samples is therefore lacking 104 residues from its N terminus and 65 residues from its C terminus.

Drs2p activation by proteolysis is not the result of Cdc50p dissociation

Cdc50 proteins are thought to play an intimate role during P4-ATPase-catalyzed lipid transport (18, 19, 34–36), and the affinity of Drs2p for Cdc50p has been suggested to fluctuate during lipid transport (18). We thus asked whether Drs2p activation could have been the result of Cdc50p dissociation from the complex after proteolysis. To be able to detect Cdc50p, we resorted to a non-cleavable His_{10}-tagged version of Cdc50p, detectable by Western blotting and co-expressed and purified together with Drs2p. This Drs2p-His_{10}-Cdc50p sample (D-$_H$C), either before or after thrombin treatment, behaved just as the one with untagged Cdc50p (D-C), judging from its sensitivity to thrombin treatment (Fig. 4*A*) and its SEC elution profile (SEC profile of D-C not shown). Subjecting the T+ species to SEC made it possible to evaluate to what extent Drs2p and Cdc50p remain associated after proteolysis. Both the intact and the T+-proteolyzed Drs2p-Cdc50p complexes only contained very few aggregates, and they eluted as sharp peaks well separated from detergent micelles or thrombin (Fig. 4*B*). For thrombin-treated samples, elution was delayed to a volume slightly larger than that for the untreated sample (but smaller than that for a solubilized SERCA1a-sarcolipin complex (37)), suggesting that most of the small fragments resulting from Drs2p proteolysis have dissociated from the large fragments, instead of remaining bound via weak interactions. Yet, Western blotting analysis of the eluted fractions clearly showed that the two subunits remained associated during SEC, for both intact and thrombin-treated D-$_H$C complexes (Fig. 4*C*).

To further strengthen our conclusion, association between proteolyzed Drs2p and His_{10}-Cdc50p was also explored by allowing His_{10}-Cdc50p to interact with a Ni^{2+} resin. For the thrombin-treated D-$_H$C complex, as for the intact D-$_H$C complex, both Drs2p and Cdc50p remained bound to the resin (Fig. 4*D*, *left*). For the untagged D-C complex, unspecific adsorption of the complex on the Ni^{2+} resin remained modest, confirming that Drs2p in the D-$_H$C complex had been fished out via the His-tagged Cdc50p, for both intact and proteolyzed samples (Fig. 4*D*, *left*). Most of the ATPase activity of the thrombin-treated D-$_H$C complex was also retained on the Ni^{2+} resin (Fig. 4*D*, *right*), thereby excluding that stimulation of activity could be due to Drs2p dissociation from its associated subunit.

Detailed characterization of the sensitivity of thrombin-treated Drs2p-Cdc50p complexes to various lipids as well as to ATP

Zhou *et al.* (28) recently showed that the transport activity of Drs2p devoid of its whole C terminus is comparable, both in the absence and presence of PI4P, with that of full-length Drs2p in the presence of PI4P, suggesting that PI4P binding relieves auto-inhibition of the pump. We therefore investigated in detail the PI4P dependence of Drs2p activity after proteolysis. Evaluating the PI4P dependence of the activity of a sample resulting from proteolysis in the *absence* of PI4P was quite straightforward, and this sample clearly retained sensitivity to PI4P (*lanes 2* and *3* in Fig. 2*B*). In contrast, evaluating the dependence on PI4P of the activity of a sample resulting from proteolysis in the *presence* of PI4P (T+) required strong dilution of the sample, to reach a low enough PI4P final concentration, and it also required us to leave sufficient time for PI4P dissociation from the diluted T+ sample, before testing the effect of back addition of PI4P. The continuous NADH-coupled assay proved here to be particularly useful, as it made it possible to show that PI4P dissociation is rather slow, with a half-time of about 5 min at 30 °C (Fig. 5*A*, *trace* (*ii*)), and that subsequent PI4P binding fully reactivates the proteolyzed sample. Thus, the T+ sample is also sensitive to PI4P. Proteolyzed samples were also found to remain sensitive to PS, with the kinetics for PS dissociation (Fig. 5*A*, *trace* (*iii*)) being slightly faster than the kinetics for PI4P dissociation.

The apparent affinity for PI4P of the T− sample, in the presence of a saturating concentration of PS, was found higher than its apparent affinity for PS in the presence of a saturating concentration of PI4P, and it was similar to that found for intact Drs2p-Cdc50p complex (Fig. 5*B*) (23). Affinities of a T+ sample for PI4P and PS were found to be similar to those of the intact and T− samples, although maximal activities were higher (Fig. 5*B* and Table 1). The stronger binding of PI4P, compared with PS, fits with the faster dissociation rate of PS (Fig. 5*A*), at least assuming comparable binding rates.

Note that the most relevant parameter to describe the effect of a particular concentration of lipid in the presence of a given concentration of detergent is the lipid/detergent ratio (or the ratio of lipid to micellar detergent, reflecting the local lipid concentration within the detergent micellar phase), rather than the lipid concentration in the aqueous volume. Indeed, results obtained under "standard" DDM concentrations (0.75–2 mg/ml) and those obtained at significantly higher DDM concentrations (3–5 mg/ml) are within error (*open versus closed symbols* for the T− species in Fig. 5*B*) if lipid concentrations are expressed as lipid/DDM ratios. In such terms, the K_m value for activation by PI4P is about 0.005 g of PI4P/g of DDM (Table 1 and Fig. 5*B*). If expressed in terms of moles of lipid/mol of detergent ratio, this corresponds to less than 1 mol of PI4P per 200 mol of DDM. We estimate that about 200 molecules of DDM surround the transmembrane region of the Drs2p-Cdc50p complex,[4] so the K_m value corresponds to less than one PI4P molecule in the immediate environment of Drs2p, emphasizing the strong affinity of the thrombin-treated Drs2p for PI4P.

Both PI4P and $PI(4,5)P_2$ have previously been shown to interact with a patch of basic residues, $RMKKQR^{1273}$, which has therefore been assigned as the binding site for PI4P on the C-terminal extension of Drs2p (27). We investigated whether other phospholipids of the inositol lipid family could stimulate Drs2p ATPase activity to the same extent as PI4P, and we found that stimulation of the activity of a Drs2p-Cdc50p thrombin-treated T− sample was specific to PI4P, as neither phosphatidylinositol nor $PI(4,5)P_2$ was

[4] C. Montigny, P. Champeil, and G. Lenoir, unpublished results.

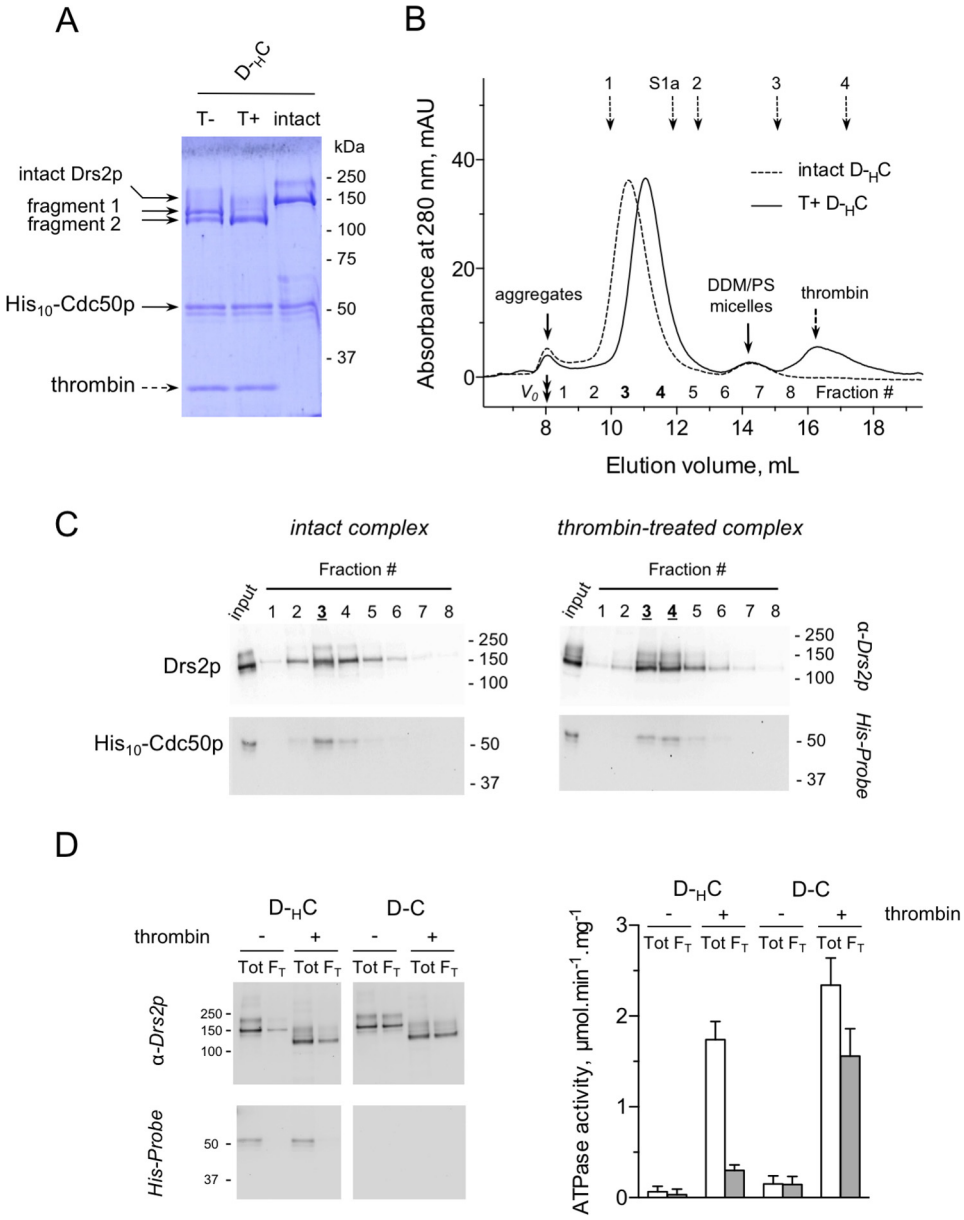

Figure 4. Cdc50p does not dissociate from Drs2p upon proteolysis by thrombin. *A*, here Drs2p has been co-expressed with a non-cleavable His-tagged version of Cdc50p (D-$_H$C). SDS-PAGE analysis of the proteolysis by thrombin of the Drs2p-His$_{10}$-Cdc50p complex (D-$_H$C), under the same conditions as those for Drs2p-Cdc50p (D-C) samples in *lanes 3* and *4* of Fig. 2 (T− and T+ samples). *B*, size-exclusion chromatography on a Superdex 200 10/300GL column, with a mobile phase containing 0.5 mg/ml DDM and 0.05 mg/ml POPS. The *double-arrow* indicates the dead volume (V_0 ~8 ml). The elution positions of standard proteins (thyroglobulin, 670 kDa (*1*), γ-globulin, 158 kDa (*2*), ovalbumin, 44 kDa (*3*), and myoglobin, 17.5 kDa (*4*)), as well as those for thrombin alone, eluting at ~16.1 ml, or a solubilized SERCA1a-sarcolipin complex, eluting at ~11.8 ml, are indicated. The injected sample was either intact Drs2p-His$_{10}$-Cdc50p (*dashed line*) or Drs2p-His$_{10}$-Cdc50p that had been pretreated with thrombin in the presence of PI4P (*T+*, *continuous line*). The SEC profiles were identical to those obtained when a Drs2p-Cdc50p (D-C) complex was used. *C*, Western blotting analysis of the fractions collected during SEC of D-$_H$C complexes, using either an antibody directed against Drs2p or a His probe. *Input* corresponds to the injected sample. The data plotted represent a typical experiment of two independent ones. *D*, thrombin-treated T+ samples (both D-$_H$C and D-C) were incubated with a Ni^{2+}-TED resin: 0.5 ml of T+ sample at 0.15 mg of protein/ml was incubated with 8.5 mg of pre-equilibrated Ni^{2+}-TED resin for 45 min at 4 °C in SSR buffer containing 0.5 mg/ml DDM, 0.025 mg/ml POPS. Unbound material was recovered by centrifugation for 5 min at 500 × *g*. Total samples (*Tot*) and flow-through (F_T) were examined by immunoblotting (*left*), as well as for their ATPase activities in the presence of PI4P (*right*). The results with untagged Cdc50p (D-C) confirm that nonspecific adsorption of Drs2p to the resin is only modest under these conditions.

effective (Fig. 5*C*). The presence of the latter lipids did not prevent subsequent activation by PI4P (data not shown).

We finally investigated the apparent affinity for ATP of the thrombin-treated T+ sample. Its K_m for Mg^{2+}-ATP was found to be ~5 μM (Fig. 5*D*), close to that previously determined for phosphorylation of the intact complex (~10 μM (23)). We found only little further activation by millimolar concentrations of Mg^{2+}-ATP (Fig. 5*D*), unlike for the Ca^{2+}-pump SERCA1a, which does show modulatory binding modes for ATP, as reported previously (33, 38–40).

Increased overall activity, in the presence of PI4P, of thrombin-treated Drs2p, correlates with a greatly stimulated rate of dephosphorylation for the Ala^{105}–Arg^{1290} polypeptide

Using a classical type of experiment in which ^{32}P-labeled phosphoenzyme is first formed from [γ-^{32}P]ATP before being

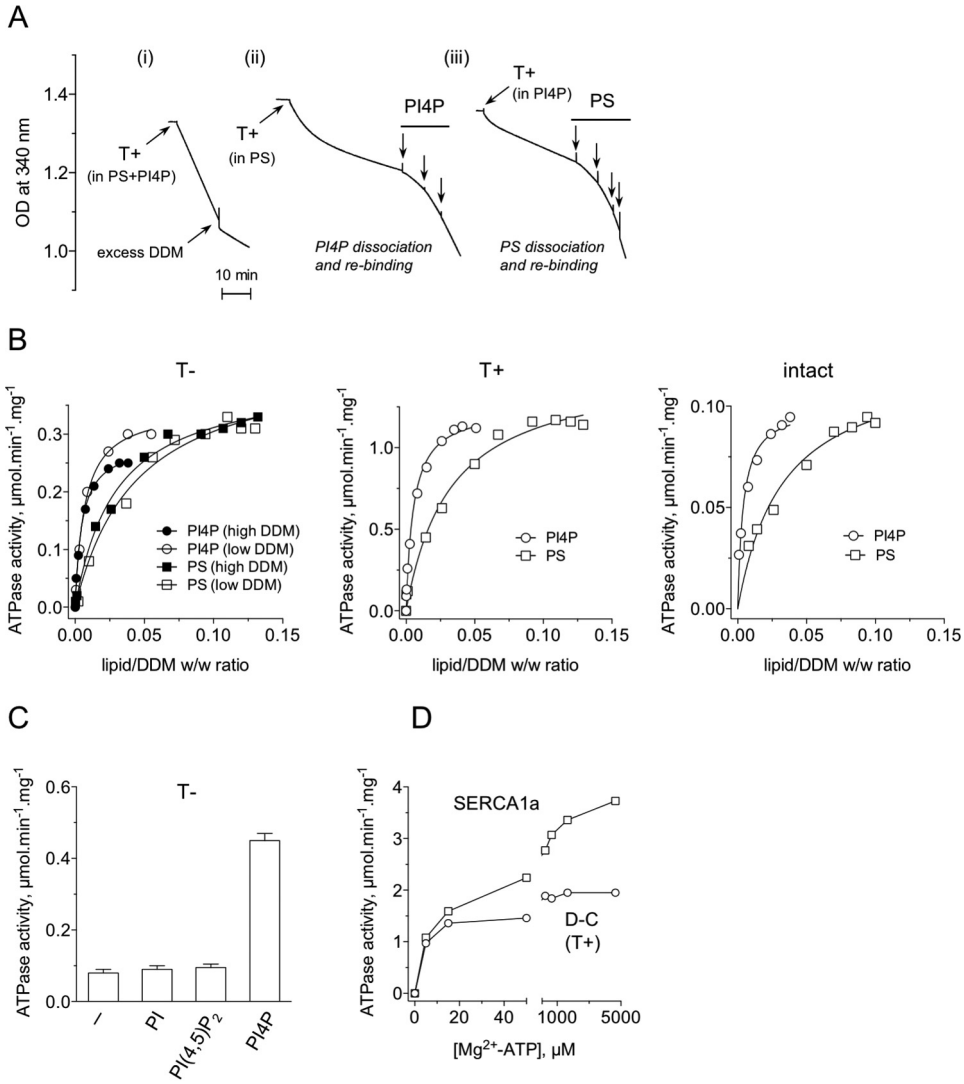

Figure 5. Characterization of the phospholipid and ATP dependence of thrombin-treated samples. ATPase activities were either measured using the enzyme-coupled assay (*A*, for the *T*− and *T*+ species in *B* and for *C* and *D*) or the phosphomolybdate procedure (for the intact complex in *B*), in the presence of a regenerating system in both cases. *A*, Drs2p-Cdc50p T+ sample was diluted 200-fold (10 μl in 2 ml) in a medium containing DDM and either PS and PI4P (*i*), or PS only (*ii*), or PI4P only (*iii*), at the following final concentrations: (i) 1 mg/ml DDM, 0.05 mg/ml PS, and 0.025 mg/ml PI4P; (ii) 0.75 mg/ml DDM and 0.05 mg/ml PS; (iii) 0.75 mg/ml DDM and 0.025 mg/ml PI4P. In (*i*), final addition of excess pure DDM micelles, up to a total DDM concentration of 4 mg/ml, resulted in a drop in enzyme activity, due to dilution of both PS and PI4P into the excess detergent. In (*ii*), PI4P was added after ~40 min delay, at concentrations of 2, 8, and then 24 μg/ml, from a stock solution containing 5 mg/ml PI4P and 50 mg/ml DDM. In (*iii*), similarly, PS was added after ~35-min delay, at final concentrations of 10, 30, 90, and 290 μg/ml from a stock solution containing 10 mg/ml PS and 50 mg/ml DDM. In the latter case, the final DDM concentration increased up to ~2.2 mg/ml. *B*, for the T− sample, K_m for PI4P was deduced from measurements performed either with low total DDM concentrations (*open circles*), 0.75–2 mg/ml, or with high total DDM concentrations (*closed circles*), 3–5 mg/ml; similarly, K_m for PS was measured either at low total DDM concentrations (*open squares*), 0.75–2.25 mg/ml, or at high total DDM concentrations (*closed squares*), 3–8 mg/ml. For the T+ sample, the K_m value for both PI4P and PS was measured at high total DDM concentrations, namely 3–5.5 mg/ml for PI4P and 3–7.5 mg/ml for PS. For the intact Drs2p-Cdc50p complex, the K_m value for both PI4P and PS was measured at 1 mg/ml total DDM concentration. In all cases, the companion lipid was kept at a saturating level. *C*, activities were measured for a thrombin-treated (T−) Drs2p-Cdc50p purified complex, in the presence of 0.025 mg/ml of various inositol phospholipid species, together with 0.1 mg/ml PS and 1 mg/ml DDM. *D*, apparent affinity for Mg^{2+}-ATP of a T+ sample (D-C), in the presence of 1 mg/ml DDM, 0.05 mg/ml PS, and 0.025 mg/ml PI4P as well as for SERCA1a from solubilized SR membranes, in the presence of 20 μM Ca^{2+}. In both cases the final concentration of ATPase was 1 μg/ml protein.

chased with excess unlabeled Mg^{2+}-ATP, we previously found that dephosphorylation of the transiently formed phosphoenzyme species of an intact Drs2p-Cdc50p complex was slow, occurring on a time scale of minutes at 30 °C. Therefore, Drs2p dephosphorylation is most probably rate-limiting for overall ATPase activity (23, 41). Phosphoenzyme formation in thrombin-treated Drs2p-Cdc50p was first measured using a filtration protocol after acid quenching. Time course of phosphorylation of the intact or thrombin-treated Drs2p-Cdc50p complex revealed that for the T− and T+ species, [γ-^{32}P]ATP was consumed very rapidly at 30 °C, as shown by the lower initial level of phosphoenzyme formed and by its rapid disappearance over time (Fig. 6*A*). This is in line with the much higher ATP hydrolysis rate of the truncated species. To prevent exhaustion of [γ-^{32}P]ATP within the 1st min while performing phosphorylation and dephosphorylation experiments with proteolyzed samples, we therefore had to turn to 4 °C (Fig. 6*A*).

For the intact Drs2p-Cdc50p complex, most of the phosphoenzyme formed remained stable over a few minutes after an ATP chase at 4 °C (Fig. 6*B*, *left*). In contrast, for a T+ sample,

Table 1

Kinetic parameters for activation of ATP hydrolysis by intact as well as thrombin-treated T− and T+ Drs2p-Cdc50p complexes

Standard errors and number of data points, *n*, on which the analysis is based, are indicated. To determine the K_m values and the maximum velocity values, data were fitted to a hyperbolic function. ND indicates not determined.

	Activation by PI4P of ATP hydrolysis at low DDM		Activation by PI4P of ATP hydrolysis at high DDM		Activation by PS of ATP hydrolysis at low DDM		Activation by PS of ATP hydrolysis at high DDM	
Drs2p/Cdc50p	K_m [a]	V_{max} [b]	K_m [a]	V_{max} [b]	K_m [a]	V_{max} [b]	K_m [a]	V_{max} [b]
Intact	0.004 ± 0.0005 $n = 7$	0.10 ± 0.003 $n = 7$	ND	ND	0.033 ± 0.003 $n = 8$	0.12 ± 0.004 $n = 8$	ND	ND
T−	0.007 ± 0.0006 $n = 6$	0.35 ± 0.008 $n = 6$	0.005 ± 0.0004 $n = 9$	0.28 ± 0.006 $n = 9$	0.044 ± 0.009 $n = 9$	0.44 ± 0.03 $n = 9$	0.029 ± 0.004 $n = 10$	0.40 ± 0.01 $n = 10$
T+	ND	ND	0.005 ± 0.0007 $n = 11$	1.25 ± 0.04 $n = 11$	ND	ND	0.032 ± 0.005 $n = 11$	1.50 ± 0.08 $n = 11$

[a] K_m is expressed in lipid/DDM g/g units.
[b] V_{max} is expressed in μmol·min^{-1}·mg^{-1} Drs2p.

the phosphoenzyme completely disappeared after the chase, within half a minute (Fig. 6*B*, *right*), consistent with the greatly increased ATPase activity of T+ samples at 4 °C (Fig. 6*A*). Remarkably, for the T− sample, only about half of the phosphoenzyme disappeared after the ATP chase, although the rest remained stable (Fig. 6*B*, *center*). In view of the fact that this T− sample contains significant amounts of both fragments 1 and 2, this suggested that one of these fragments might dephosphorylate quickly, although the other retained slow dephosphorylation, almost as slow as for the intact Drs2p-Cdc50p complex.

To distinguish between fragment 1 and fragment 2 as regards their ability to undergo phosphorylation and dephosphorylation, we subjected phosphorylated and ATP-chased samples to electrophoretic separation on acidic gels, *i.e.* under conditions that retain the otherwise alkali-labile acylphosphate bond of the phosphoenzyme (42). In these experiments (Fig. 6*C*), the smaller of the two proteolytic fragments found in a T− sample, as well as the quasi-unique fragment found in a T+ sample (the Ala^{105}–Arg^{1290} polypeptide in both cases), exhibited greatly increased dephosphorylation rates, whereas the rate of dephosphorylation of the larger fragment in T− (the Ala^{105}–Ile^{1355} polypeptide) was essentially as slow as that for untreated Drs2p. These experiments clearly show that C-terminal cleavage of Drs2p at Arg^{1290} is required to significantly accelerate dephosphorylation of the transient phosphoenzyme intermediate, consistent with the apparent correlation between stimulation of the overall ATPase activity and formation of the proteolytic fragment 2 (compare *lanes 3* and *4* in Fig. 2, *A* and *B*).

To confirm that N-terminal cleavage of the first 104 residues of Drs2p alone is not sufficient for accelerating dephosphorylation of the transiently formed phosphoenzyme in fragment 1, we used a Drs2p preparation highly enriched in a Drs2p polypeptide lacking its first 104 residues (ΔN104, see "Experimental procedures"). MALDI-TOF analysis of this sample confirmed that it mainly corresponded to fragment 105–1355 (data not shown). This ΔN104 form had an ATPase activity at 30 °C only moderately higher than that of the full-length Drs2p (*open symbols* in Fig. 6*D*), and we could therefore perform phosphorylation and dephosphorylation experiments at 30 °C. As displayed in Fig. 6*D*, the kinetics of dephosphorylation for the main component of this ΔN104 preparation was essentially similar to that for full-length Drs2p, as revealed either by filtration experiments or after electrophoretic separation (Fig. 6*D*). Thus, the slightly faster rate of ATP hydrolysis by the ΔN104 form was probably only due to the presence of a small amount of a shorter form of Drs2p, apparently dephosphorylating much more rapidly (*dotted arrow* in Fig. 6*D*, *right*), a fraction contributing to ATPase activity much more than it does to the phosphoenzyme level. Because ΔN104 has been recovered from streptavidin beads by treatment with thrombin, this minor Drs2p form might in fact be cleaved at Arg^{1290}, too. Our results therefore indicate that solely removing the first 104 residues of Drs2p may alter slightly, but not much, the functional properties of the Drs2p-Cdc50p complex, whereas the concomitant removal of 65 C-terminal residues greatly stimulates its ATPase activity.

Removing only 53 residues from the C terminus (1303–1355) is not sufficient to fully stimulate Drs2p activity

We then asked whether removing only the C-terminal end of Drs2p would be sufficient to relieve auto-inhibition of the complex. Toward this goal, we generated various C-terminally shortened versions of Drs2p, based on the putative contents and organization of Drs2p C-terminal region (26). Specifically, we selected variants (Fig. 7*A*, *left*) ending either immediately after the putative transmembrane segment 10 (Tyr^{1226}), before or after the Gea2p/PI4P-binding site (Ser^{1249} and Arg^{1273}, respectively) or after the Vps36p homology domain (Gly^{1283}), or, finally, at a position (Gly^{1302}) thought to be similar to that of the C-terminal amino acid of ATP8A2, a mammalian P4-ATPase that displays a very high ATP hydrolysis rate (24).

We first looked at the ability of these shortened variants to complement the cold-sensitive growth defect of Δ*drs2* yeast cells. Although the ΔC1302 variant could complement this growth defect, further deletions up to amino acid 1226 were unable to do so (Fig. 7*A*, *right*), suggesting that deletion beyond Gly^{1302} is detrimental to Drs2p activity. In subsequent co-expression attempts, we found that all variants were expressed, although in some cases at levels significantly lower than for wild-type Drs2p, including for the ΔC1302 variant (data not shown), and in some cases with altered Cdc50p glycosylation pattern. In addition, all variants turned out to be poorly solubilized by DDM, so that the purification yield of the various deletions turned out to be limited compared with wild-type Drs2p (data not shown).

We thus continued with the ΔC1302 variant and compared its properties with those of wild-type enzyme. The purified ΔC1302 variant was phosphorylated to a fair extent compared with full-length enzyme. Nevertheless, the more rapid exhaus-

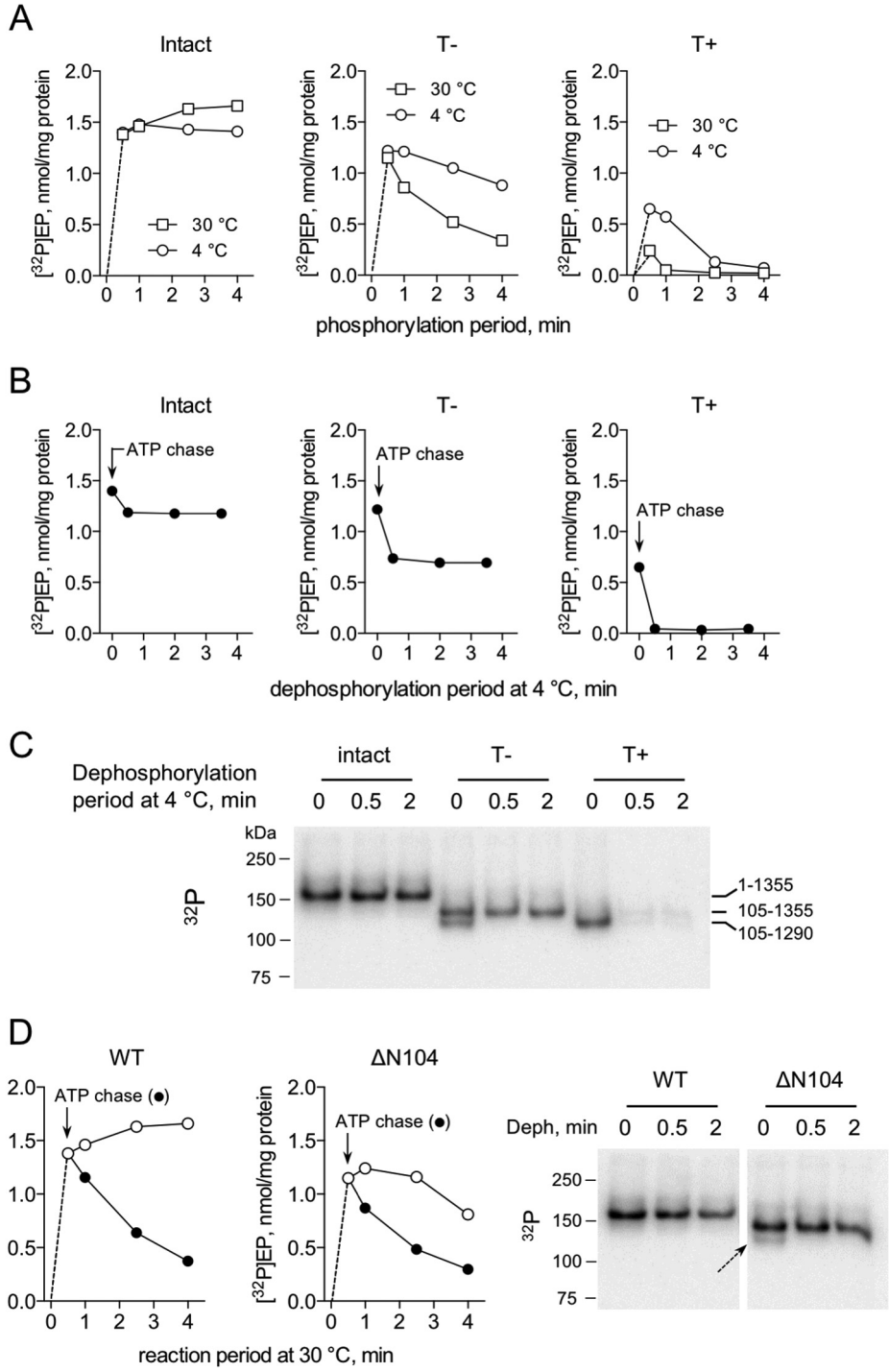

Figure 6. Ala^{105}–Arg^{1290} Drs2p fragment, but not the Ala^{105}–Ile^{1355} fragment, displays a largely increased dephosphorylation rate. Intact Drs2p-Cdc50p, T−, or T+ samples, diluted to 10 μg/ml in SSR with 1 mg/ml DDM, 0.05 mg/ml PS, and 0.025 mg/ml PI4P, were supplemented with 2 μM [γ-^{32}P]ATP for phosphorylation and subsequent dephosphorylation after an ATP chase. *A*, time course of phosphorylation, at either 4 or 30 °C. The reaction was quenched after various periods of time, and radioactivity was measured by scintillation counting. The *dotted lines* indicate that the phosphorylation kinetics have not been measured at very short times. *B*, following 0.5 min of phosphorylation at 4 °C, the time course of dephosphorylation after an ATP chase was measured, as followed by filtration after acid quenching and scintillation counting. *C*, similar phosphorylation and dephosphorylation experiment, but now followed by loading quenched samples onto an acidic gel and imaging the various radioactive bands in a PhosphorImager. *D*, phosphorylation and dephosphorylation of either the intact Drs2p-Cdc50p complex or a ΔN104 fragment, as measured here at 30 °C, either after acid quenching and filtration (*left, open symbols* for phosphorylation and *closed symbols* for dephosphorylation after ATP chase) or after separation of the phosphorylated bands on acidic gels and radioactivity imaging (*right*). The *dotted lines* indicate that the phosphorylation kinetics have not been measured at very short times.

tion of ATP by ΔC1302 (*open symbols* in Fig. 7*B*, *left*) suggested that its hydrolysis rate was faster than that of the full-length enzyme, as also suggested by ATPase activity measurements (*histograms* in Fig. 7*C*). The half-time of dephosphorylation of the ΔC1302 variant was indeed shorter than for the full-length enzyme, but only 2-fold shorter, as deduced from both filtration experiments (*closed symbols* in Fig. 7*B*, *left*) or after electrophoretic separation (Fig. 7*B*, *right*). Thus, deletion of the final 53

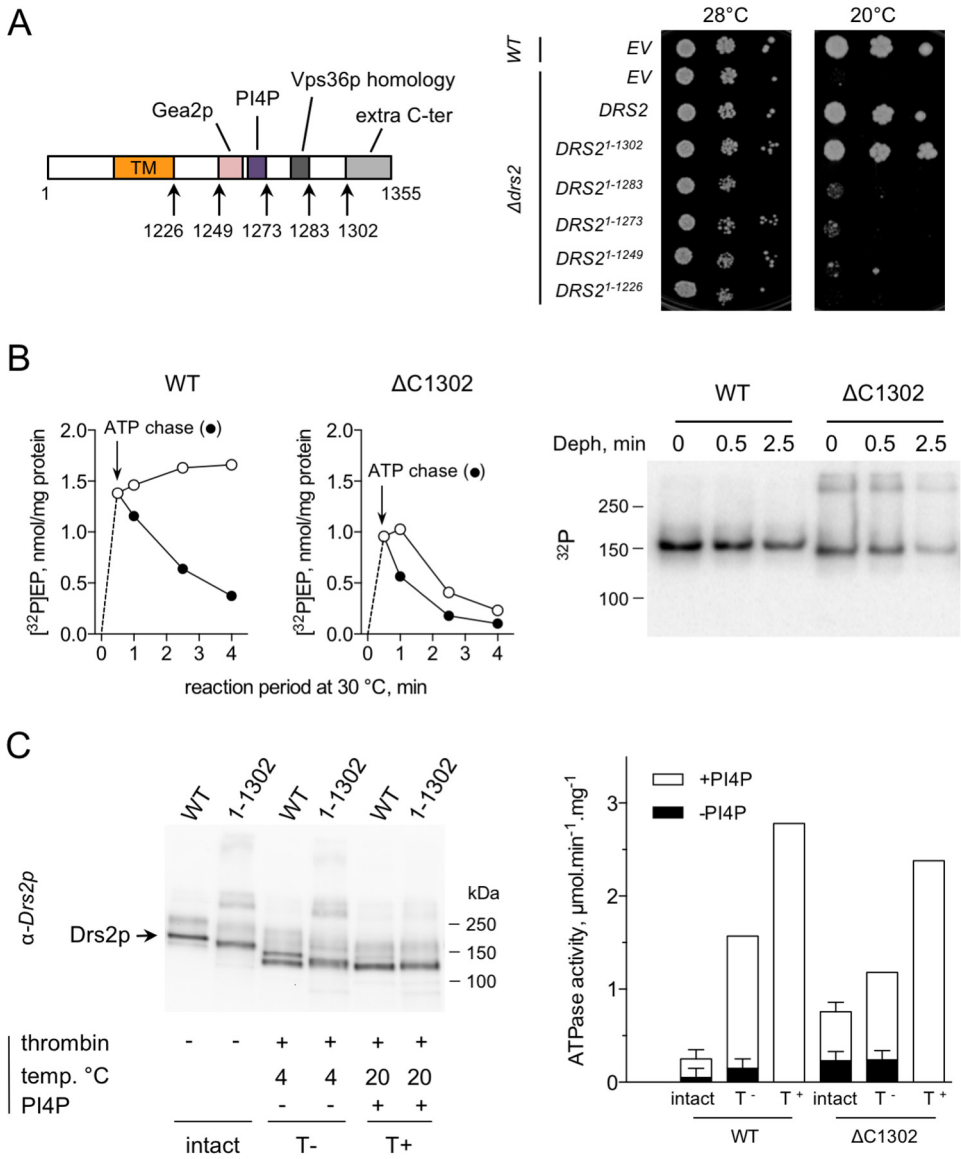

Figure 7. Removing C-terminal residues 1303–1355 stimulates Drs2p activity only weakly. *A*, *left,* end-points selected for expression of various C-terminally shortened Drs2p variants; *extra C-ter* refers to the extreme C terminus of Drs2p, which has no equivalent in the mammalian ATP8A2; *right*, restoration of the cold-sensitive growth defect of Δ*drs2* cells by plasmid-borne Drs2 variants. In this case, Drs2p was expressed in the absence of Cdc50p. Serial yeast dilutions were spotted on S5A medium in the presence of 1% fructose (23). *B*, phosphorylation and dephosphorylation of wild-type Drs2p-Cdc50p complex or a ΔC1302 truncated variant. Time course of phosphorylation and dephosphorylation was measured at 30 °C, either after acid quenching and filtration (*left, open symbols* for phosphorylation and *closed symbols* for dephosphorylation after ATP chase) or after separation of the phosphorylated bands on acidic gels and radioactivity imaging (*right*). The N-terminally BAD-tagged 1–1302 Drs2p variant was co-expressed with Cdc50p, purified, and diluted to about the same protein concentration as a wild-type Drs2p. The *dotted lines* indicate that time 0 of phosphorylation has not been measured in this case. *C*, removal by thrombin of residues 1–104 in the purified ΔC1302 variant results in a modest increase of its activity. The ΔC1302 variant, as well as the WT complex, was submitted to thrombin treatment in the absence (T−) or presence (T+) of PI4P. *Left,* Western blotting analysis, using an α-Drs2p antibody, of WT and ΔC1302, either before (intact) or after treatment with thrombin in the absence (T−) or presence (T+) of PI4P. *Right,* ATPase activity of the same samples, measured in the absence (*closed bars*) or presence (*open bars*) of PI4P.

residues of Drs2p does stimulate its ATPase activity, but only moderately, significantly less than the activation achieved for the Ala^{105}–Arg^{1290} polypeptide. Proteolysis by thrombin of the ΔC1302 variant occurred in a manner similar to that for wild type, with cleavage in the presence of PI4P (T+) apparently resulting in the same 105–1290 polypeptide as for wild type, and with concomitant increase in ATPase activity (Fig. 7*C*). Notably, proteolysis of the 1–1302 variant under T− conditions only resulted in a modest relative increase in activity (Fig. 7*C*, *right*), showing that the Ala^{105}–Gly^{1302} polypeptide anticipated to be formed after the T− treatment is less active than the Ala^{105}–Arg^{1290} polypeptide. Taken together, these results suggest that the 1291–1302 region, when intact, maintains significant auto-inhibition of Drs2p, irrespective of the absence or presence of the N-terminal 1–104 residues.

We wondered whether the sole truncation of the C-terminal region, including the 1291–1302 region, would be sufficient for fully activating Drs2p. However, cleavage by thrombin in the N terminus of Drs2p occurs prior to cleavage at its C terminus, making it impossible to isolate a polypeptide devoid of its C-terminal residues only. Therefore, we generated a Drs2p variant in which the Arg^{104} residue, the site of N-terminal thrombin

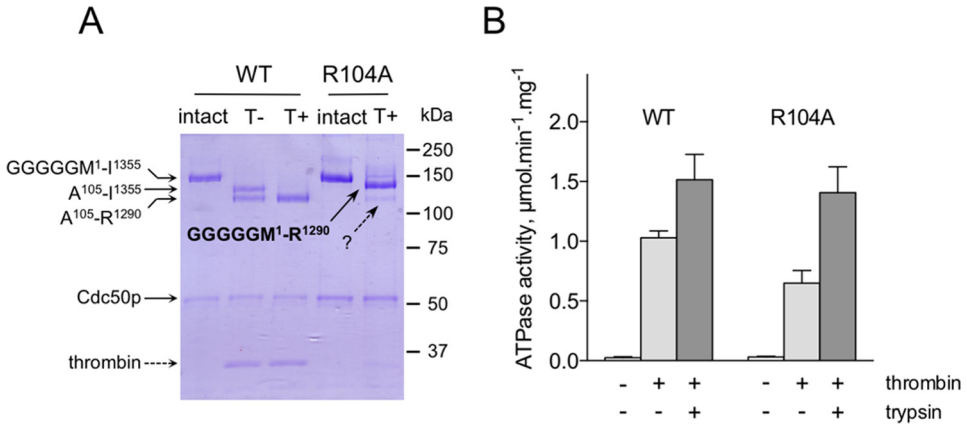

Figure 8. N- and C-terminal extensions cooperate for Drs2p-Cdc50p auto-inhibition. *A*, Coomassie Blue-stained SDS-PAGE after treatment of WT or the R104A variant with thrombin, in the absence (T−) or presence (T+) of PI4P. The *?* underlines the uncertainty as to the identity of the polypeptide running with the same velocity as the Ala^{105}–Arg^{1290} fragment, obtained by proteolysis with thrombin of the wild-type complex. *B*, removing residues 1291–1355 of Drs2p R104A by a thrombin T+ treatment yields major but not full activation of the complex. Samples treated with thrombin in the presence of PI4P (T+ conditions) were subjected to ATPase activity measurements, in a medium containing PS and PI4P, using an enzyme-coupled assay. Trypsin was added to the cuvette at the end of the measurement, as a control of the maximal velocity that can be reached for both wild-type and R104A species. The *histograms* represent the specific activity calculated from the rate of NADH oxidation. Data are presented as the mean ± S.D. *Error bars* are of two to eight independent experiments.

cleavage, has been swapped with an alanine. The R104A variant of Drs2p-Cdc50p was then subjected to proteolysis by thrombin in the presence of PI4P (T+) to obtain a Drs2p polypeptide truncated at Arg^{1290} only. SDS-PAGE analysis of R104A limited proteolysis confirmed that we obtained the anticipated C-terminally truncated form (Fig. 8*A*), with only a residual amount of a shorter Drs2p form, probably truncated on both sides, *i.e.* at Arg^{1290} as well as at some arginine residue close to Arg^{104}. As displayed in Fig. 8*B*, removing the C-terminal sequence of Drs2p positioned between Met^{1291} and Ile^{1355} upon treatment of the R104A variant with thrombin, in the presence of PI4P, did stimulate ATPase activity to a significant extent, but not as much as that observed upon treatment of wild-type Drs2p-Cdc50p with thrombin. Subsequent incubation with trypsin ascertained that the R104A variant nevertheless had the potential to reach the same maximal rate of ATP hydrolysis as that of the wild type. From this, we conclude that although truncation at Arg^{1290} in the C terminus has more of a significant effect than truncation at Arg^{104} in the N terminus, solely removing the C terminus of Drs2p is not sufficient to achieve full activation of the complex; together with the C-terminal region, the N terminus of Drs2p probably also contributes auto-inhibitory constraints.

Discussion

Removal of Drs2p C- and N-terminal extensions stimulates its ATPase activity: general comments

We demonstrate here that limited proteolysis of Drs2p, down to polypeptides with sizes only slightly larger than that of its central core, dramatically increases its ATP hydrolysis rate. Such stimulation is achieved upon proteolysis with various proteases, including thrombin and trypsin (Figs. 1 and 2). At least in the case of proteolysis by thrombin, stimulation of ATPase activity unambiguously appears to be associated with truncation of N- and C-terminal extensions down to the major polypeptide occurring after cleavage under T+ conditions (Figs. 2 and 6).

This T+ Drs2p fragment was identified by N-terminal sequencing and MALDI-TOF (Fig. 3) mass spectrometry as mostly consisting of Drs2p cleaved at a single N-terminal position (after Arg^{104}) and a single C-terminal position (after Arg^{1290}), namely the Ala^{105}–Arg^{1290} fragment. This Drs2p large polypeptide remained associated with Cdc50p, and the complex eluted as a homogeneous peak in gel filtration experiments (Fig. 4), with the smaller Stokes radius compared with that of the intact complex implying that the small Drs2p fragments resulting from proteolysis have dissociated from the complex.

The fact that Drs2p activity can be stimulated by proteolysis unambiguously confirms the insightful suggestion by Graham's lab that the full-length Drs2p-Cdc50p complex is an auto-inhibited enzyme (28). As Cdc50p remains intact during proteolysis by thrombin (Fig. 2), this auto-inhibition must be conveyed by the Drs2p extensions themselves. Because the N- and C-terminal extensions of Drs2p were trimmed off preferentially upon proteolysis, it is likely that these portions of Drs2p are especially exposed or disordered in the full-length protein.

What are the critical regions involved in auto-inhibition? Although we currently have only partial answers to this question, a clear fact is that trimming off the N-terminal first 104 residues only, as in fragment 1 or in the ΔN104 truncated form of Drs2p, is not sufficient for stimulating turnover (Fig. 6) and that deleting the C-terminal last 53 residues only, as in the 1–1302 Drs2p variant, is only poorly efficient (Fig. 7*B*). Further deletion of residues 1–104 in this 1–1302 Drs2p variant does not fully stimulate ATPase activity either (Fig. 7*C*). Similarly, removing only the last 65 C-terminal residues (from Met^{1291} to Ile^{1355}) does not yield full activation of the Drs2p-Cdc50p complex; the intact R104A variant, when treated with thrombin, displays an ATPase activity significantly lower (by ~30%) than that of the wild type treated with thrombin (Fig. 8). Hence, the results presented in this study point to a possible cooperation between the N- and C-terminal extensions of Drs2p in the auto-inhibition process. Further work is needed to clarify this point

in detail, but regulation of Drs2p-Cdc50p by both termini would be reminiscent of the inhibition mechanism described for other P-type ATPases, the plant H^+-ATPase and the yeast H^+-ATPase (32, 43). Irrespective of such possible cooperation between the two termini, what is clear is that trimming off both the N-terminal 1–104 residues and the C-terminal 1291–1355 residues or only the C-terminal 1291–1355 residues substantially relieves auto-inhibition (Figs. 2, 4–6, and 8). Thus, removing the segment encompassed by residues 1291–1302 on the C-terminal side appears to be critical for significant stimulation of Drs2p activity. In other words, truncation must apparently come rather close to the putative PI4P-binding site (ending at Arg^{1273}) to become effective. Similarly, N-terminal truncation might have to be more extensive than the mere deletion of residues 1–104 to become effective by itself. In this regard, it is worth noting that the Arl1p-binding site, starting at Asp^{153} on the N-terminal extension of Drs2p, is indeed located closer to the central core of Drs2p than the Arg^{104} residue.

The present data also allow us to suggest that the very low activity previously found for the purified Drs2p-Cdc50p complex (23) reflects the presence of a quasi-intact C terminus, and, conversely, that a Drs2p-Cdc50p preparation with high ATPase activity might well contain a significant fraction of a C-terminally truncated enzyme, as suspected previously (28). Such a situation is exemplified by our result with the ΔN104 form (Fig. 6*D*). Incidentally, these data also suggest that for P-type ATPases exhibiting intrinsically low ATPase activity, phosphoenzyme measurements are probably more appropriate than the usual simple ATPase measurements for initial detection of intact forms of these P-type ATPases in crude membranes, and for their subsequent purification.

Of course, we still have to investigate whether upon proteolysis ATPase activity is coupled to lipid transport, the putative main function of the Drs2p-Cdc50p complex. This has to be determined in the near future. Then, if ATP hydrolysis by the un-inhibited enzyme is indeed coupled to lipid transport, why would yeast need such a high lipid transport activity? We might speculate here that in resting conditions, the turnover rate of Drs2p-Cdc50p is fairly slow, as suggested by the fact that PS seems to be transported quite slowly in yeast TGN or secretory vesicle membranes (20, 21). Conversely, a high lipid transport rate might be required in some specific instances, *e.g.* when the demand in vesicular trafficking (promoted by PS translocation by Drs2p) between the various cell organelles is high. This view is substantiated by the fact that PI4P is mandatory, even after removal of N- and C-terminal extensions, for activation of the uninhibited Drs2p-Cdc50p complex.

Stimulated ATPase activity of proteolyzed samples retains sensitivity to PI4P and PS: possible implications for the mechanism underlying auto-inhibition relief

Our results show that thrombin cleavage of Drs2p down to the Ala^{105}–Arg^{1290} fragment results in a species that not only displays a clearly increased ATPase activity but also retains the typical PS and PI4P dependence (Figs. 2 and 5) previously found for the intact Drs2p-Cdc50p complex (23). Therefore, our results provide renewed light on the auto-inhibition phenomenon previously identified by Zhou *et al.* (28).

The data collected by these authors showed that deletion of 121 residues from the C-terminal end of Drs2p (from Thr^{1234} to the end, which includes removal of the PI4P-binding site) resulted in a lipid transport activity that was independent of PI4P but comparable with that of the intact enzyme in the presence of PI4P. In contrast, we find that after thrombin treatment the PI4P-dependent ATPase activity increases greatly, by ~10–20-fold (Figs. 1, 2, and 5). Thus, it now appears that by deleting from the C terminus between 53 residues (Drs2p ending at Gly^{1302}) and 121 residues (Drs2p ending at Thr^{1234}), and by simultaneously deleting part of the N terminus, it is possible to greatly increase the maximal activity of Drs2p without losing the stimulatory effect of PI4P, while also retaining the ability to discriminate between PI4P and other phosphoinositides (Fig. 5*D*). In other words, the previously proposed auto-inhibition of Drs2p does not only apply to the particular state adopted by Drs2p in the absence of its lipid regulator, PI4P, but it more widely applies to intact Drs2p, the activity of which, even in the presence of PI4P, is kept remarkably low compared with what can be observed once inhibitory constraints have been released.

From a mechanistic point of view, the fact that Drs2p truncated down to the Ala^{105}–Arg^{1290} fragment remains sensitive to PI4P means that stimulation exerted by PI4P binding is not mediated by some sort of displacement of the very ends of Drs2p, namely the Met^1–Arg^{104} and Arg^{1291}–Ile^{1355} segments. We may rather envision that binding of PI4P displaces segments closer to the central core of Drs2p, like the Arg^{1273}–Arg^{1290} segment, thereby inducing conformational changes in the pump that eventually stimulate the dephosphorylation step of the transport cycle. In relation to this, the fact that proteolysis of Drs2p to fragment 2 (Fig. 2) was made faster by PI4P supports the idea that PI4P probably loosens the interaction of the polypeptide chain around Arg^{1290} with the central core of Drs2p.

Our data suggest a multistep model for how Drs2p auto-inhibition by its terminal extensions can be relieved. In a first step, a critical segment in the C terminus, beyond the PI4P-binding site (possibly in the 1273–1302 region), would need to be displaced from some inhibitory site. Based on the large size of the N- and C-terminal ends, we speculate that this inhibitory site might be located within or at the interface between the large A-, N-, and P-soluble domains. Conceivably, constraints dependent on the permanent binding of this critical segment within its binding site, a binding that might be stabilized by the additional presence of the N-terminal extension, could indeed restrict motions of the cytoplasmic domains, and thereby prevent fast dephosphorylation of Drs2p. In line with the latter hypothesis, we observed that stimulation of the ATPase activity upon thrombin treatment is associated with the large increase in the dephosphorylation rate for the Ala^{105}–Arg^{1290} proteolytic fragment (Fig. 6). The mechanism by which this critical segment could be displaced from this auto-inhibitory position remains unknown, but Gea2p and/or Arl1p, which have been shown to interact with the Drs2p C and N termini, respectively (25, 26), might possibly fulfill this role, alone or in concert. In a second step, PI4P binding would now be able to fully exert its stimulatory role, the preliminary displacement of the Drs2p C terminus making activation by PI4P much more potent (the

converse might also be true, namely that PI4P binding first primes the pump for subsequent Arl1p/Gea2p binding). This view is supported by the fact that addition of both PI4P and Gea2p to purified TGN membranes was shown to provide synergistic activation of Drs2p (27). From a physiological perspective, multistep activation could provide a tighter control on the flippase activity, by restricting lipid transport to TGN membranes where PI4P and Gea2p/Arl1p are located (44, 45).

Experimental procedures

Materials

Thrombin (bovine) was from Calbiochem (604980, >2000 units/mg). Trypsin (T1005, >6000 units/mg) was from Sigma. DDM (D310) was from Anatrace, and PI4P (840045P) and POPS (840024P), sometimes only noted here as PS, were from Avanti Polar Lipids. Drs2p was detected using an anti-Drs2p antibody (kind gift of Dr. Todd Graham), and His-tagged Cdc50p was detected using a His probe.

Expression and purification of wild-type Drs2p-Cdc50p complex and related mutants

Deletions and single point mutations were introduced into *DRS2* using standard techniques and were verified by sequencing on the entire coding sequence. N-terminal biotin acceptor domain (BAD)-tagged Drs2p and His_{10}-tagged Cdc50p were expressed in *Saccharomyces cerevisiae* membranes from a single co-expression pYeDP60 plasmid, as described in (23, 46). Wild-type Drs2p-Cdc50p complex and variants were affinity-purified on streptavidin beads, as described previously (23), except that protease inhibitors were omitted from the resin washing steps. The complexes were released from the resin by TEV cleavage, in SSR buffer (50 mM MOPS-Tris, pH 7.0, 100 mM KCl, 5 mM $MgCl_2$, 20% glycerol) containing 0.5 mg/ml DDM and 0.025 mg/ml POPS. The protein concentration in the purified fractions was in the 0.12–0.32 mg/ml range, depending on whether a second purification step on a Ni^{2+}-TED resin was included or not (to eliminate the His-tagged TEV protease). In some cases (Fig. 4), experiments were performed with purified material obtained after co-expression of wild-type BAD-tagged Drs2p with Cdc50p lacking the cleavage site between the decahistidine tag and Cdc50p ($D\text{-}_{H}C$).

The ΔN104 form was purified after co-expression with Cdc50p of a full-length Drs2p construct comprising a C-terminal BAD tag preceded by a cleavage site for thrombin, using in this case a Δ*pep4* yeast strain, built on W303-1a (*MATa, leu2-3, 112trp1-1 can1-100 ura3-1 ade2-1 his3-11,15*). ΔN104 protein samples were purified similarly to the wild-type form with minor modifications. Streptavidin-bound Drs2p-Cdc50p complexes, in protease inhibitor-free (except during membrane solubilization) SSR buffer + 0.5 mg/ml DDM and 0.025 mg/ml POPS, was cleaved from the resin overnight with 25 units (4 units/ml resin) of thrombin at 4 °C. The eluate was subsequently collected and concentrated to ~10 mg/ml and purified using SEC-FPLC on a TSK G4000SW using an Äkta purifier system at 4–10 °C with SSR + 0.5 mg/ml DDM as mobile phase. Fractions were collected, pooled, and concentrated to 2–2.4 mg/ml and snap-frozen in liquid nitrogen. N-terminal sequencing experiments revealed that thrombin had in fact cleaved the Drs2p construct not only at its inserted cleavage site, but also at another location within the Drs2p sequence, after Arg^{104}.

Limited proteolysis

For most experiments in this report, DDM and POPS were added to purified Drs2p-Cdc50p complex in its SSR buffer with minimal dilution, up to 1 mg/ml and 0.05 mg/ml, respectively, and if relevant together with 0.025 mg/ml PI4P. Proteolysis with thrombin or trypsin was performed at 20 °C and was triggered by addition of a concentrated protease suspension (*e.g.* at 10- or 100-fold the desired final concentration) to a final concentration of 40 units/ml or 40 μg/ml, respectively. The only exception to this protocol was for the R104A variant, which was treated with 15 units/ml thrombin. Proteolysis took place for various periods. At the end, the protease was quenched with minimal dilution, generally by adding a final concentration of 2 mM PMSF (quenching with 2 mM PMSF was generally faster than quenching with a commercial mixture of inhibitors) or, for the experiments with trypsin, with twice as much (w/w) trypsin inhibitor. The quenched aliquots were either used immediately or flash-frozen in liquid nitrogen before subsequent use.

For SDS-PAGE analysis of the proteolytic fragments obtained after quenching the protease with PMSF, 10-μl aliquots of the protein samples were mixed with 10 μl of urea-containing loading buffer and heated at 30 °C for 10 min. When trypsin proteolysis had been stopped with trypsin inhibitor, samples were heated for 1 min at 96 °C to prevent reactivation of trypsin in SDS-PAGE loading buffer. In all cases, samples were loaded onto either 10 or 8% acrylamide gels.

SEC analysis

For SEC-FPLC, samples were run on an Äkta purifier system at 8–12 °C, on a Superdex 200 10/300 GL column (GE Healthcare, France). About 500 μl of purified complexes at 150 μg/ml were injected. The mobile phase contained 50 mM MOPS-Tris, pH 7.0, 100 mM KCl, 5 mM $MgCl_2$, 0.5 mg/ml DDM, and 0.05 mg/ml POPS. Both the wild-type complex (D-C) and $D\text{-}_{H}C$ were submitted to such SEC, with or without preliminary proteolysis treatment. Fractions collected after SEC, as well as initial input samples at ~150 μg/ml total protein, were loaded onto an 8% SDS-PAGE for subsequent immunoblot analysis. Either 3 μl of the input sample (~135 ng of protein, *i.e.* ~100 ng of Drs2p and 35 ng of Cdc50p) or 20 μl of the collected fractions were loaded.

ATPase activity measurements

Two different protocols were used. First, the rate of ATP hydrolysis was monitored continuously at 340 nm via its coupling to NADH oxidation (thanks to the presence of pyruvate kinase, lactate dehydrogenase, phosphoenolpyruvate, and NADH (33)). In these experiments, 10–40 μl of the purified Drs2p-Cdc50p complex, resulting in final concentrations of 0.6–6 μg/ml in the various experiments, was generally added to a cuvette already containing 2 ml of the ATPase assay medium, which consisted of SSR supplemented with DDM as well as with POPS, PI4P, or other lipids (concentrated lipid/DDM stock solutions were typically 10 mg/ml POPS or 5 mg/ml

PI4P in 50 mg/ml DDM), at 30 °C. In all cases, addition of ADP at a final concentration of 10 μM led to the expected oxidation of 10 μM NADH (resulting in a fast OD change of ~0.06 AU at 340 nm). Conversion from NADH oxidation rates expressed in mAU/s to ATPase activities expressed in μmol·min^{-1}·mg^{-1} was based on the extinction coefficient of NADH at 340 nm (~6 mM^{-1}·cm^{-1}). For most experiments, photobleaching of NADH was reduced by inserting an MTO J310A filter that eliminates the short wavelength UV-exciting light of our diode-array spectrophotometer lamp, as excitation of the 260-nm absorption band of NADH is much more deleterious for light stability of NADH than excitation of its 340-nm band. This setup reduced the spontaneous rate of NADH absorption changes down to ~0.01 mAU/s and made it possible to detect the very low activities of untreated Drs2p-Cdc50p complexes. NADH absorption traces have not been corrected for the small changes due to dilution.

Second, liberated P_i was directly detected thanks to its chromogenic reaction with molybdate (23), after the ATP hydrolysis reaction was quenched with SDS at given time points (33 μl of reaction medium was mixed with 17 μl of 10% SDS). This protocol can monitor long reaction periods with small assay volumes in a 96-well plate format, possibly with high concentrations of purified samples, and it is effective for characterizing very low ATPase activities, as found in non-proteolyzed complexes. For such measurements, the purified Drs2p-Cdc50p complexes were generally diluted only ~3-fold in the final assay medium.

Data corresponding to a typical experiment of several similar ones were generally plotted with a confidence error bar (*e.g.* in Figs. 2 and 3).

Phosphoenzyme formation from [γ-^{32}P]ATP and turnover-dependent dephosphorylation

For phosphorylation experiments, [γ-^{32}P]ATP was added to the purified complex. Typically, 10 μl of [γ-^{32}P]ATP at 20 μM and about 100 μCi/ml were added to 90 μl of ice-cold protein at 11 μg/ml, and samples were then either left on ice or transferred to 30 °C. After the desired period, the reaction was quenched under stirring by diluting 10-μl aliquots into 1 ml of acid solution containing 500 mM TCA and 30 mM H_3PO_4. After about 1 h aggregation on ice of the denatured proteins, samples were filtered on GSWP Millipore filters, extensively rinsed with acid (diluted 10-fold compared with the quenching solution), and counted by scintillation.

For dephosphorylation experiments (ATP chase), excess nonradioactive Mg^{2+}-ATP was added to the sample after 30 s or 1 min of phosphorylation (typically, 10 μl of Mg^{2+}-ATP at 20 mM was added to the 100 μl of protein now at 10 μg/ml and 2 μM [γ-^{32}P]ATP), and after the desired period of subsequent turnover and therefore hydrolysis of the radioactive phosphoenzyme, 11-μl aliquots were acid-quenched as before and filtered.

Using the intact Drs2p-Cdc50p complex, we had previously found that because of the very slow rate of ATP hydrolysis, phosphorylation and dephosphorylation experiments were best done at 30 °C, with phosphoenzyme turnover then occurring over a few minutes (23). In the present experiments, however, [γ-^{32}P]ATP at an initial concentration of 2 μM was rapidly exhausted by protease-treated Drs2p-Cdc50p complexes at 30 °C (Fig. 6). In such situations, to prevent complete exhaustion of [γ-^{32}P]ATP within the 1st min, we followed phosphorylation and dephosphorylation at 4 °C.

To study phosphorylation or dephosphorylation of the individual protein fragments after their electrophoretic separation, the phosphorylation reaction was quenched by diluting aliquots 1:1 into a urea- and SDS-containing quenching medium, and quenched samples were loaded onto a "Sarkadi" gel (42, 47), to avoid hydrolysis of the radioactive phosphoenzyme. Typically, 16 μl of sample at 10 μg protein/ml was mixed with 16 μl of a twice-concentrated loading buffer (300 mM Tris-HCl, pH 6.8, 4% SDS, 8 M urea, 20% glycerol, 20 mM EDTA, and 1.4 M β-mercaptoethanol), and 20 μl of this mixture was loaded onto a Sarkadi gel. The stacking gel contained 4% acrylamide, 65 mM Tris-H_3PO_4, pH 5.5, 0.1% SDS, 0.4% ammonium persulfate, and 0.2% TEMED, and the separating gel was a continuous 7% gel, containing 65 mM Tris-H_3PO_4, pH 6.5, 0.1% SDS, 0.4% ammonium persulfate, and 0.05% TEMED. Gels were run in the cold room, and the pre-cooled running buffer contained 0.1% SDS and 170 mM MOPS-Tris, pH 6.0. Dried gels were subsequently stained with Coomassie Blue (or analyzed by Western blotting) before radioactivity of the various bands was measured, using PhosphorImager equipment.

N-terminal sequencing

Proteolytic fragments separated on SDS-PAGE were transferred onto a PVDF membrane. The membrane was rinsed with water and then with 10% methanol for a few seconds before staining with Coomassie Blue in 1% acetic acid and 40% methanol. The membrane was then rapidly rinsed in water alone, before the colored bands for the various fragments were excised and dried. Sequencing of the amino acids resulting from N-terminal Edman degradation was performed using an Applied Biosystems gas-phase sequencer model 492. Phenylthiohydantoin amino acid derivatives generated at each sequence cycle were identified and quantitated on-line with an Applied Biosystems Model 140C HPLC system using the data analysis system for protein sequencing from Applied Biosystems (software Procise PC version 2.1). Chromatography was used to identify and quantify the derivatized amino acid removed at each sequence cycle.

Mass spectrometry

Truncated fragments of SEC-purified Drs2p were identified by MALDI-TOF mass spectrometry, as described previously for the intact Drs2p-Cdc50p complex (23).

Author contributions—H. A., C. M., P. C., and G. L. performed most of the experiments and analyzed the data. T. D. performed experiments investigating the effect of proteolysis on Drs2p-Cdc50p association and purified the E342Q mutant. A. J. initiated the construction of truncated versions of Drs2p. P. L. M. performed MALDI-TOF experiments. J. L. V. I. provided assistance with mass spectrometry experiments and edited the manuscript. J. U., M. R. A., and J. A. L. identified conditions to obtain Drs2p truncated at Arg^{104} and purified it. M. R. A., P. N., and J. A. L. analyzed the data and edited the manuscript. G. L. designed the study, and G. L. and P. C. wrote the manuscript. All authors reviewed the results and approved the final version of the manuscript.

Acknowledgments—We thank Paulette Decottignies for help with mass spectrometry experiments, Maylis Lejeune for help with the purification of the Arg^{104} variant, Todd Graham for generously providing the α-Drs2p antibody, Rosa López-Marqués for providing the Δpep4 strain, and Jean-Pierre Andrieu, from the platform of the Partnership for Structural Biology at the Institut de Biologie Structurale in Grenoble (PSB/IBS) for the N-terminal sequencing experiments. We also thank Anant Menon for advice concerning the organization of the manuscript and Marc le Maire for stimulating discussions.

References

1. Sanyal, S., and Menon, A. K. (2009) Flipping lipids: why an' what's the reason for? *ACS Chem. Biol.* **4,** 895–909
2. Menon, I., Huber, T., Sanyal, S., Banerjee, S., Barré, P., Canis, S., Warren, J. D., Hwa, J., Sakmar, T. P., and Menon, A. K. (2011) Opsin is a phospholipid flippase. *Curr. Biol.* **21,** 149–153
3. Goren, M. A., Morizumi, T., Menon, I., Joseph, J. S., Dittman, J. S., Cherezov, V., Stevens, R. C., Ernst, O. P., and Menon, A. K. (2014) Constitutive phospholipid scramblase activity of a G protein-coupled receptor. *Nat. Commun.* **5,** 5115
4. Malvezzi, M., Chalat, M., Janjusevic, R., Picollo, A., Terashima, H., Menon, A. K., and Accardi, A. (2013) Ca^{2+}-dependent phospholipid scrambling by a reconstituted TMEM16 ion channel. *Nat. Commun.* **4,** 2367
5. Zhou, Y., Wong, C.-O., Cho, K. J., van der Hoeven, D., Liang, H., Thakur, D. P., Luo, J., Babic, M., Zinsmaier, K. E., Zhu, M. X., Hu, H., Venkatachalam, K., and Hancock, J. F. (2015) SIGNAL TRANSDUCTION. Membrane potential modulates plasma membrane phospholipid dynamics and K-Ras signaling. *Science* **349,** 873–876
6. Yeung, T., Heit, B., Dubuisson, J.-F., Fairn, G. D., Chiu, B., Inman, R., Kapus, A., Swanson, M., and Grinstein, S. (2009) Contribution of phosphatidylserine to membrane surface charge and protein targeting during phagosome maturation. *J. Cell Biol.* **185,** 917–928
7. Fadok, V. A., Voelker, D. R., Campbell, P. A., Cohen, J. J., Bratton, D. L., and Henson, P. M. (1992) Exposure of phosphatidylserine on the surface of apoptotic lymphocytes triggers specific recognition and removal by macrophages. *J. Immunol.* **148,** 2207–2216
8. Tang, X., Halleck, M. S., Schlegel, R. A., and Williamson, P. (1996) A subfamily of P-type ATPases with aminophospholipid transporting activity. *Science* **272,** 1495–1497
9. van der Mark, V. A., Elferink, R. P., and Paulusma, C. C. (2013) P4 ATPases: flippases in health and disease. *Int. J. Mol. Sci.* **14,** 7897–7922
10. Onat, O. E., Gulsuner, S., Bilguvar, K., Nazli Basak, A., Topaloglu, H., Tan, M., Tan, U., Gunel, M., and Ozcelik, T. (2013) Missense mutation in the ATPase, aminophospholipid transporter protein ATP8A2 is associated with cerebellar atrophy and quadrupedal locomotion. *Eur. J. Hum. Genet.* **21,** 281–285
11. López-Marqués, R. L., Poulsen, L. R., Bailly, A., Geisler, M., Pomorski, T. G., and Palmgren, M. G. (2015) Structure and mechanism of ATP-dependent phospholipid transporters. *Biochim. Biophys. Acta.* **1850,** 461–475
12. Montigny, C., Lyons, J., Champeil, P., Nissen, P., and Lenoir, G. (2016) On the molecular mechanism of flippase- and scramblase-mediated phospholipid transport. *Biochim. Biophys. Acta* **1861,** 767–783
13. Baldridge, R. D., and Graham, T. R. (2013) Two-gate mechanism for phospholipid selection and transport by type IV P-type ATPases. *Proc. Natl. Acad. Sci. U.S.A.* **110,** E358–E367
14. Baldridge, R. D., and Graham, T. R. (2012) Identification of residues defining phospholipid flippase substrate specificity of type IV P-type ATPases. *Proc. Natl. Acad. Sci. U.S.A.* **109,** E290–E298
15. Vestergaard, A. L., Coleman, J. A., Lemmin, T., Mikkelsen, S. A., Molday, L. L., Vilsen, B., Molday, R. S., Dal Peraro, M., and Andersen, J. P. (2014) Critical roles of isoleucine-364 and adjacent residues in a hydrophobic gate control of phospholipid transport by the mammalian P4-ATPase ATP8A2. *Proc. Natl. Acad. Sci. U.S.A.* **111,** E1334–E1343
16. Saito, K., Fujimura-Kamada, K., Furuta, N., Kato, U., Umeda, M., and Tanaka, K. (2004) Cdc50p, a protein required for polarized growth, associates with the Drs2p P-type ATPase implicated in phospholipid translocation in *Saccharomyces cerevisiae*. *Mol. Biol. Cell.* **15,** 3418–3432
17. Chen, S., Wang, J., Muthusamy, B.-P., Liu, K., Zare, S., Andersen, R. J., and Graham, T. R. (2006) Roles for the Drs2p-Cdc50p complex in protein transport and phosphatidylserine asymmetry of the yeast plasma membrane. *Traffic* **7,** 1503–1517
18. Lenoir, G., Williamson, P., Puts, C. F., and Holthuis, J. C. (2009) Cdc50p plays a vital role in the ATPase reaction cycle of the putative aminophospholipid transporter Drs2p. *J. Biol. Chem.* **284,** 17956–17967
19. Takahashi, Y., Fujimura-Kamada, K., Kondo, S., and Tanaka, K. (2011) Isolation and characterization of novel mutations in CDC50, the non-catalytic subunit of the Drs2p phospholipid flippase. *J. Biochem.* **149,** 423–432
20. Natarajan, P., Wang, J., Hua, Z., and Graham, T. R. (2004) Drs2p-coupled aminophospholipid translocase activity in yeast Golgi membranes and relationship to *in vivo* function. *Proc. Natl. Acad. Sci. U.S.A.* **101,** 10614–10619
21. Alder-Baerens, N., Lisman, Q., Luong, L., Pomorski, T., and Holthuis, J. C. (2006) Loss of P4 ATPases Drs2p and Dnf3p disrupts aminophospholipid transport and asymmetry in yeast post-Golgi secretory vesicles. *Mol. Biol. Cell.* **17,** 1632–1642
22. Zhou, X., and Graham, T. R. (2009) Reconstitution of phospholipid translocase activity with purified Drs2p, a type-IV P-type ATPase from budding yeast. *Proc. Natl. Acad. Sci. U.S.A.* **106,** 16586–16591
23. Azouaoui, H., Montigny, C., Ash, M.-R., Fijalkowski, F., Jacquot, A., Grønberg, C., López-Marqués, R. L., Palmgren, M. G., Garrigos, M., le Maire, M., Decottignies, P., Gourdon, P., Nissen, P., Champeil, P., and Lenoir, G. (2014) A high-yield co-expression system for the purification of an intact Drs2p-Cdc50p lipid flippase complex, critically dependent on and stabilized by phosphatidylinositol-4-phosphate. *PloS One* **9,** e112176,
24. Coleman, J. A., Vestergaard, A. L., Molday, R. S., Vilsen, B., and Andersen, J. P. (2012) Critical role of a transmembrane lysine in aminophospholipid transport by mammalian photoreceptor P4-ATPase ATP8A2. *Proc. Natl. Acad. Sci. U.S.A.* **109,** 1449–1454
25. Tsai, P.-C., Hsu, J.-W., Liu, Y.-W., Chen, K.-Y., and Lee, F.-J. (2013) Arl1p regulates spatial membrane organization at the trans-Golgi network through interaction with Arf-GEF Gea2p and flippase Drs2p. *Proc. Natl. Acad. Sci. U.S.A.* **110,** E668–E677
26. Chantalat, S., Park, S.-K., Hua, Z., Liu, K., Gobin, R., Peyroche, A., Rambourg, A., Graham, T. R., and Jackson, C. L. (2004) The Arf activator Gea2p and the P-type ATPase Drs2p interact at the Golgi in *Saccharomyces cerevisiae*. *J. Cell Sci.* **117,** 711–722
27. Natarajan, P., Liu, K., Patil, D. V., Sciorra, V. A., Jackson, C. L., and Graham, T. R. (2009) Regulation of a Golgi flippase by phosphoinositides and an ArfGEF. *Nat. Cell Biol.* **11,** 1421–1426
28. Zhou, X., Sebastian, T. T., and Graham, T. R. (2013) Auto-inhibition of Drs2p, a yeast phospholipid flippase, by its carboxyl-terminal tail. *J. Biol. Chem.* **288,** 31807–31815
29. Curran, A. C., Hwang, I., Corbin, J., Martinez, S., Rayle, D., Sze, H., and Harper, J. F. (2000) Autoinhibition of a calmodulin-dependent calcium pump involves a structure in the stalk that connects the transmembrane domain to the ATPase catalytic domain. *J. Biol. Chem.* **275,** 30301–30308
30. Baekgaard, L., Fuglsang, A. T., and Palmgren, M. G. (2005) Regulation of plant plasma membrane H+- and Ca^{2+}-ATPases by terminal domains. *J. Bioenerg. Biomembr.* **37,** 369–374
31. Lopreiato, R., Giacomello, M., and Carafoli, E. (2014) The plasma membrane calcium pump: new ways to look at an old enzyme. *J. Biol. Chem.* **289,** 10261–10268
32. Ekberg, K., Palmgren, M. G., Veierskov, B., and Buch-Pedersen, M. J. (2010) A novel mechanism of P-type ATPase autoinhibition involving both termini of the protein. *J. Biol. Chem.* **285,** 7344–7350
33. Møller, J. V., Lind, K. E., and Andersen, J. P. (1980) Enzyme kinetics and substrate stabilization of detergent-solubilized and membranous (Ca^{2+} + Mg^{2+})-activated ATPase from sarcoplasmic reticulum. Effect of protein-protein interactions. *J. Biol. Chem.* **255,** 1912–1920

34. Coleman, J. A., and Molday, R. S. (2011) Critical role of the beta-subunit CDC50A in the stable expression, assembly, subcellular localization, and lipid transport activity of the P4-ATPase ATP8A2. *J. Biol. Chem.* **286,** 17205–17216
35. Bryde, S., Hennrich, H., Verhulst, P. M., Devaux, P. F., Lenoir, G., and Holthuis, J. C. (2010) CDC50 proteins are critical components of the human class-1 P4-ATPase transport machinery. *J. Biol. Chem.* **285,** 40562–40572
36. Poulsen, L. R., López-Marqués, R. L., McDowell, S. C., Okkeri, J., Licht, D., Schulz, A., Pomorski, T., Harper, J. F., and Palmgren, M. G. (2008) The *Arabidopsis* P4-ATPase ALA3 localizes to the Golgi and requires a β-subunit to function in lipid translocation and secretory vesicle formation. *Plant Cell* **20,** 658–676
37. Montigny, C., Decottignies, P., Le Maréchal, P., Capy, P., Bublitz, M., Olesen, C., Møller, J. V., Nissen, P., and le Maire, M. (2014) *S*-Palmitoylation and *S*-oleoylation of rabbit and pig sarcolipin. *J. Biol. Chem.* **289,** 33850–33861
38. Champeil, P., le Maire, M., Andersen, J. P., Guillain, F., Gingold, M., Lund, S., and Møller, J. V. (1986) Kinetic characterization of the normal and detergent-perturbed reaction cycles of the sarcoplasmic reticulum calcium pump. Rate-limiting step(s) under different conditions. *J. Biol. Chem.* **261,** 16372–16384
39. Clausen, J. D., McIntosh, D. B., Anthonisen, A. N., Woolley, D. G., Vilsen, B., and Andersen, J. P. (2007) ATP-binding modes and functionally important interdomain bonds of sarcoplasmic reticulum Ca^{2+}-ATPase revealed by mutation of glycine 438, glutamate 439, and arginine 678. *J. Biol. Chem.* **282,** 20686–20697
40. Clausen, J. D., McIntosh, D. B., Woolley, D. G., and Andersen, J. P. (2008) Critical interaction of actuator domain residues arginine 174, isoleucine 188, and lysine 205 with modulatory nucleotide in sarcoplasmic reticulum Ca^{2+}-ATPase. *J. Biol. Chem.* **283,** 35703–35714
41. Jacquot, A., Montigny, C., Hennrich, H., Barry, R., le Maire, M., Jaxel, C., Holthuis, J., Champeil, P., and Lenoir, G. (2012) Phosphatidylserine stimulation of Drs2p·Cdc50p lipid translocase dephosphorylation is controlled by phosphatidylinositol-4-phosphate. *J. Biol. Chem.* **287,** 13249–13261
42. Lenoir, G., Picard, M., Gauron, C., Montigny, C., Le Maréchal, P., Falson, P., Le Maire, M., Møller, J. V., and Champeil, P. (2004) Functional properties of sarcoplasmic reticulum $Ca^{(2+)}$-ATPase after proteolytic cleavage at Leu119–Lys120, close to the A-domain. *J. Biol. Chem.* **279,** 9156–9166
43. Mason, A. B., Kardos, T. B., and Monk, B. C. (1998) Regulation and pH-dependent expression of a bilaterally truncated yeast plasma membrane H+-ATPase. *Biochim. Biophys. Acta* **1372,** 261–271
44. Balla, T. (2013) Phosphoinositides: tiny lipids with giant impact on cell regulation. *Physiol. Rev.* **93,** 1019–1137
45. Chantalat, S., Courbeyrette, R., Senic-Matuglia, F., Jackson, C. L., Goud, B., and Peyroche, A. (2003) A novel Golgi membrane protein is a partner of the ARF exchange factors Gea1p and Gea2p. *Mol. Biol. Cell* **14,** 2357–2371
46. Azouaoui, H., Montigny, C., Jacquot, A., Barry, R., Champeil, P., and Lenoir, G. (2016) Coordinated overexpression in yeast of a P4-ATPase and its associated Cdc50 subunit: The case of the Drs2p-Cdc50p lipid flippase complex. *Methods Mol. Biol.* **1377,** 37–55
47. Sarkadi, B., Enyedi, A., Földes-Papp, Z., and Gárdos, G. (1986) Molecular characterization of the in situ red cell membrane calcium pump by limited proteolysis. *J. Biol. Chem.* **261,** 9552–9557